Research Requirements Document

Fundamental Studies in Droplet Combustion and Flame Extinguishment in Microgravity (FLEX-2)

Research Team Lead:
Forman A. Williams, University of California, San Diego

NASA Research Team Members:
Daniel Dietrich, NASA Glenn Research Center
Michael Hicks, NASA Glenn Research Center
Peter M. Struk, NASA Glenn Research Center
Vedha Nayagam, National Center for Space Exploration Research

External Research Team Members:
C. Thomas Avedisian, Cornell
Mun Y. Choi, Drexel University
Frederick L. Dryer, Princeton University
Benjamin D. Shaw, University of California, Davis

Project Scientist:
Michael Hicks, NASA Glenn Research Center

November 21, 2007

Contents

List of Figures

List of Tables

1 Introduction

Combustion, which has been both friend and foe to mankind since antiquity, still defies comprehension in many important respects. Needs therefore exist to advance fundamental knowledge in combustion science. Practical consequences of such advancement of knowledge are improvements in strategies for energy production, since most of the energy that is used by society will continue to be provided by combustion for many years, and mitigation of fire losses, fire safety being a continuing concern in all sectors. The NASA Microgravity Combustion Science Program, which was established through recognition of these needs, did much to increase our fundamental understanding of combustion processes Ronney (1988),Williams (2007). Droplet combustion experiments had a great deal to do with the advancements in knowledge through this program. Such experiments, in effect, focus on a microcosm of the field of combustion that can be used to study most aspects of the topic. In addition, droplet combustion is of practical interest in itself, since liquid fuels possess high energy content per unit mass and are relatively safe to store and transport, making them valuable to the transportation industry for the foreseeable future. Phenomena of finite-rate gas-phase chemistry, multicomponent-species gas-phase transport processes, production of soot and other pollutants, phase-change processes, liquid-phase species separation and fluid motion, natural and force convection, radiation and conductive energy transfer and interactions of different burning fuel elements, for example, all are involved in droplet combustion (and, in fact, all are aspects of the subject of the present SRD). By offering a well-controlled arena in which to investigate these combustion phenomena, microgravity droplet combustion research provides valuable data that help develop detailed chemical and physical models of combustion phenomena.

The NASA program in the area of microgravity droplet combustion has employed laboratory experiments, low-gravity facilities, aircraft flying parabolic trajectories and space-based research to reduce or eliminate buoyancy, thereby increasing the fidelity of the descriptions of the combustion processes. Following glovebox space-shuttle experiments on a fiber-supported droplet combustion, FSDC, the freely deployed droplet-combustion experiment DCE was flown on the MSL-1 missions, providing a number of new insights into the fundamentals of droplet combustion. Among the DCE results was the demonstration of boundaries between radiative and diffusive extinction of combustion in droplet burning and the establishment of atmospheres in which the dilution was great enough that the oxygen concentration was too low for combustion to occur Nayagam et al. (1998), Ackerman et al. (2003). This last observation demonstrated how droplet-combustion studies could be used to investigate the limiting oxygen index, LOI, needed to prevent combustion, and so the Flammability-limit experiment FLEX, was designed for the International Space Station, ISS, to be run using the multiuser droplet combustion apparatus, MDCA, in the combustion integrated rack, CIR. While FLEX is focussed on spacecraft fire safety and fire suppression, FLEX-2 returns to the broader objective of improving the fundamental understanding of liquid-fuel combustion. The FLEX-2 experiments thus fall in the category of the broad NASA mission to improve basic science through microgravity research. They focus on ethanol and decane as fuels, as well as various fuel mixtures, in oxygen-nitrogen and oxygen-helium atmospheres at various pressures.

Specific aspects of FLEX-2 and of how the FLEX-2 plans build on and differ from previous fundamental droplet-combustion studies are addressed in detail in the following sections. Brief descriptions of the relevant literature will be given, the objectives of the proposed research effort will be outlined, descriptions will be given of the experimental research, and requirements for the flight experiments will be stated. Post-flight data analysis, ground-based efforts in support of the flight experiments and the overall science management plan are described in the subsequent sections.

2 Literature Review

2.1 Fundamentals of Pure Fuel -Droplet Combustion and Extinction

The spherically symmetrical combustion of a liquid fuel droplet in a quiescent ambient gaseous oxidizing atmosphere is a classical problem in combustion research, having been addressed first more than 50 years ago by Godsave (1952), Hall and Diederichsen (1953) and Spalding (1953b,a). Numerous reviews of the subject are now available in the literature, among them those of Wise and Agoston (1958), Williams, F. (1965), Williams (1973),Faeth (1977), Law (1982), Sirignano (1993, 1999), Avedisian (2000), Chiu (2000) and Choi and Dryer (2001). An advantage of the spherical symmetry is that only one spatial dimension enters the description of the combustion process, so that one-dimensional (spherically symmetrical) time-dependent conservation equations apply, greatly facilitating both computational and theoretical descriptions of the combustion and thereby enhancing understanding of experimental results, which becomes much more difficult, uncertain and inaccurate in multidimensional situations. Natural convection, however, destroys the spherical symmetry of the combustion in normal gravity, as was quite evident already in the earliest experiments of Hall and Diederichsen (1953) and Goldsmith (1956). Kumagai (1956) was the first to realize that microgravity experiments afforded the opportunity to achieve spherical symmetry, a fact which NASA has used to advantage in fundamental investigations for a number of years e.g., (Williams, 1981; Dietrich et al., 1996; Nayagam et al., 1998). Although microgravity experiments are, in a sense, somewhat artificial for earthbound combustion, they are of direct concern for combustion hazards in the spacecraft which are needed to pursue human exploration of planets and their satellites in space.

Despite the simplifications afforded by spherical symmetry, many complexities remain in microgravity studies of droplet combustion. Among them are time-dependent liquid-phase phenomena, soot production, radiant energy transfer and effects of multicomponent fuels. These topics are addressed in the following subsections. The focus of the present subsection is on gas-phase phenomena, as they influence burning rates and finite-rate chemistry, leading ultimately to extinction of the spherical flame that surrounds the liquid droplet. Because of the small value of the ratio of gas density to liquid density, in a first approximation the gas phase is quasisteady Williams (1960, 1985). It is this quasisteadiness, along with a fast-chemistry approximation, that leads to the well-known "d-square law" for the droplet burning rate, in which the square of the droplet diameter decreases linearly with time. There are, however, notable time-dependent gas-phase phenomena in need of further study, even when the gas-phase chemistry is fast.

One such phenomena is the flame-diameter history. An entirely quasisteady gas phase with rapid chemistry maintains a constant ratio of flame diameter to droplet diameter during combustion, but already in early microgravity droplet-combustion experiments this was observed not to occur Kumagai and Isoda (1956); Isoda and Kumagai (1958); Okajima and Kumagai (1974a). It is now understood that whether the flame diameter should behave in a quasisteady manner depends on the value of the stoichiometric mixture fraction, the ratio of the oxidizer mass to the sum of the fuel and oxidizer mass in a stoichiometric mixture (Crespo and Liñan (1975); Waldman (1974); Williams (1985)). A quasisteady flame radius occurs if the stoichiometric mixture fraction is sufficiently large, but in most experiments it is too small (less than 0.1) for the flame radius to achieve quasisteady behavior during the droplet lifetime. Dilution of the atmosphere reduces the stoichiometric mixture fraction, as does oxygenation of the fuel, so methanol, for example, in increased-oxygen atmospheres would have a more nearly quasisteady flame radius than hydrocarbon fuels, such as heptane, burning in air. Microgravity experiments (e.g., Dietrich et al. (1996)) suggest a stronger tendency toward quasisteady flame-diameter behavior for methanol than for heptane.

It is not known, however, whether this tendency also would be exhibited by ethanol, since ethanol is not as highly oxygenated as methanol. The proposed experiments with ethanol would help to address this question; for the experiments with decane, the flame diameters should remain unsteady during the entire burning history.

Microgravity experiments have shown that there always is an initial period during which the flame diameters increase with time (Nayagam et al. (1998)). During this period the flame resides in the outer transient-diffusive zone (Crespo and Liñan (1975)). Only at sufficiently large stoichiometric mixture fractions can it return to the inner convective-diffusive zone and become quasisteady. A tendency for the flame to return, that is, for the flame diameter to begin to decrease with time, can be observed only if the gas-phase chemistry remains sufficiently fast. If the chemistry is too slow, the flame may extinguish before it begins to return.

Heat losses reduce the temperature of the gas and thereby slows the chemistry. Two types of heat losses are diffusive, that is, by heat conduction away from the flame, and radiative, that is radiant energy loss from the flame region to the surroundings. Diffusive losses are increased at small flame diameters, while radiative losses are increased at large flame diameters relative to energy release. Flame extinction that occurs as the flame diameter begins to decrease after reaching a maximum is therefore termed radiative extinction, while extinctions that occurs at small flame diameters are termed diffusive extinction. The boundary between conditions of radiative and diffusive extinction depends on the initial droplet diameter and on the dilution of the atmosphere, as well as on the fuel. Microgravity experiments (Nayagam et al. (1998), Ackerman et al. 2003) have established these boundaries for heptane. The boundaries between radiative and diffusive extinction are, however, not known for ethanol or decane. The proposed experiments would determine these boundaries for these two fuels, each of which is of interest, the first as a constituent of biofuels and the second as a constituent of surrogate fuels for diesel and aircraft fuels.

Detailed chemical kinetic mechanisms are available for the combustion of both ethanol and decane fuels. It is now possible to use this detailed chemistry in time-dependent, spherically symmetrical computations of droplet burning to calculate extinction conditions. However, systematically reduced chemistry models using rate-ratio asymptotics are not yet available for these fuels. Experimental measurement of diffusive and radiative extinction boundaries for the two fuels should help in developing these reduced chemical kinetic schemes.

2.2 Liquid-Phase Phenomena

The bulk of the isolated droplet combustion studies, as seen from the previous section, treat the droplet as being a pure, single component liquid. In contrast, practical fuels are multi-component, or have constituents with a wide range of physical and chemical properties. The gas-phase and thus flame behaviors are determined by the species that have gasified, and liquid behaviors are determined by the species that remain inside of the droplets. A particular species within a droplet can be gasified only if it is present at the liquid surface. Thus, the gas phase and vaporization behaviors of a fuel droplet are strongly influenced by the rate at which various components are transported to the surface of the droplet. Previous work shows that liquid species diffusion rates are very important in determining the gasification behaviors of multicomponent droplets (see, e.g., Hanson et al. (1982); Randolph et al. (1986); Dwyer, 1989; Megaridis (1993); Sirignano (1999)).

A species can reach the surface of the droplet by two mechanisms, diffusion and convection. The causes of internal liquid convection were typically thought to result from the atomization or injection processes and the aerodynamic shear stresses at the droplet surface (Sirignano (1999)). Aharon and Shaw (1996) showed that capillary stresses can promote or oppose droplet internal flows, depending on the relative strengths of the solutal and thermal capillary stresses. These

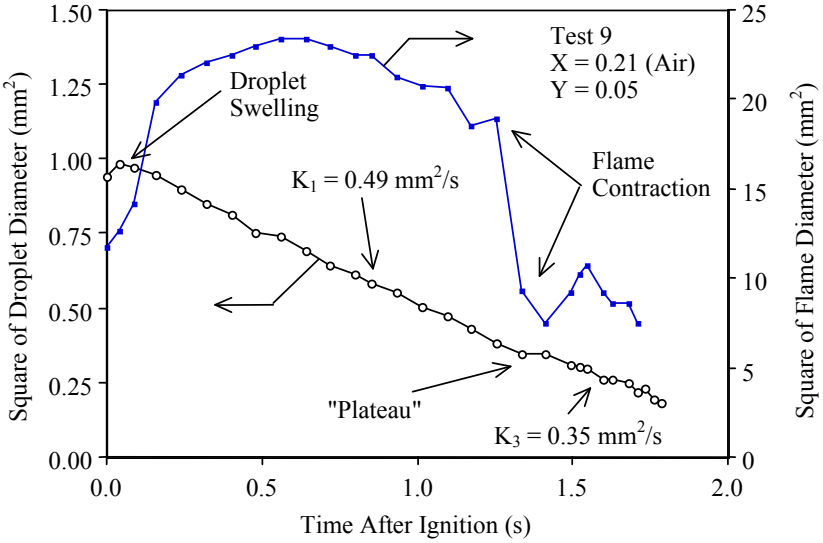

Figure 1: Representative data on droplet and flame dimensions in a microgravity combustion experiment with heptane-hexadecane droplets. In this experiment, the pressure was one atm. Data are from Aharon and Shaw (1998).

capillary stresses can dominate the internal flows and can cause strong random internal motions with spray-size droplets (50 to 100 μm or smaller), even under high droplet velocity conditions representative of modern combustors (Dwyer et al. (1996); Dwyer et al. (1998); Niazmand et al. (1995)). One of the focuses of the present FLEX-2 experiments will be to investigate the effects of thermal and solutal capillary flows on droplet combustion behaviors.

The process of differential vaporization of a bi-component fuel is manifested in the gas phase as 'flame contraction.' Flame contractions occur as a result of the massive liquid heating (and decreased vaporization) when the surface mass fraction of the low-volatility component rapidly approaches unity. Representative flame and droplet data from Aharon and Shaw (1998) showing a flame contraction are presented in Fig. 1.

Theoretical expressions have been developed (Shaw and Williams (1990)) and extended (Aharon and Shaw (1998)) to analyze conditions leading to the onset of flame contractions. The theory predicts that the ratio of the initial droplet diameter, d_0, to the droplet diameter at the onset of flame contraction, d_c, is a function of both the initial mass fraction of the low-volatility component in the droplet, Y, and the parameter $\varepsilon = 8D/K$. This parameter (ε) is the ratio of a characteristic droplet lifetime to a characteristic species diffusion time in a droplet. The variable D is the liquid species diffusivity and K is the burning-rate constant prior to the flame contraction. Under typical conditions, $\varepsilon << 1$ is expected; the theory capitalizes on the smallness of ε. The solid lines in Fig. 2 show theoretical predictions of $(d_c/d_0)^3$ as a function of Y for various values of ε.

Figure 3 shows the effective liquid phase species diffusion coefficients, D, computed from the experiments in Fig. 2. The data in Fig. 3 show that the smallest D values were in the drop tower experiments. In addition, the 0.1 MPa data show that the D values calculated from the normal-gravity results of Wang et al. (1984) are about an order-of-magnitude larger than the one-atm D values obtained by Shaw and co-workers. Clearly, the different methods used for droplet deployment influences the extent of liquid phase mixing, and thus the effective D, in many of the studies cited here. The present FLEX-2 experiments using bi-component mixtures will allow the droplet internal circulation to decay prior to ignition and characterize the motion that results from

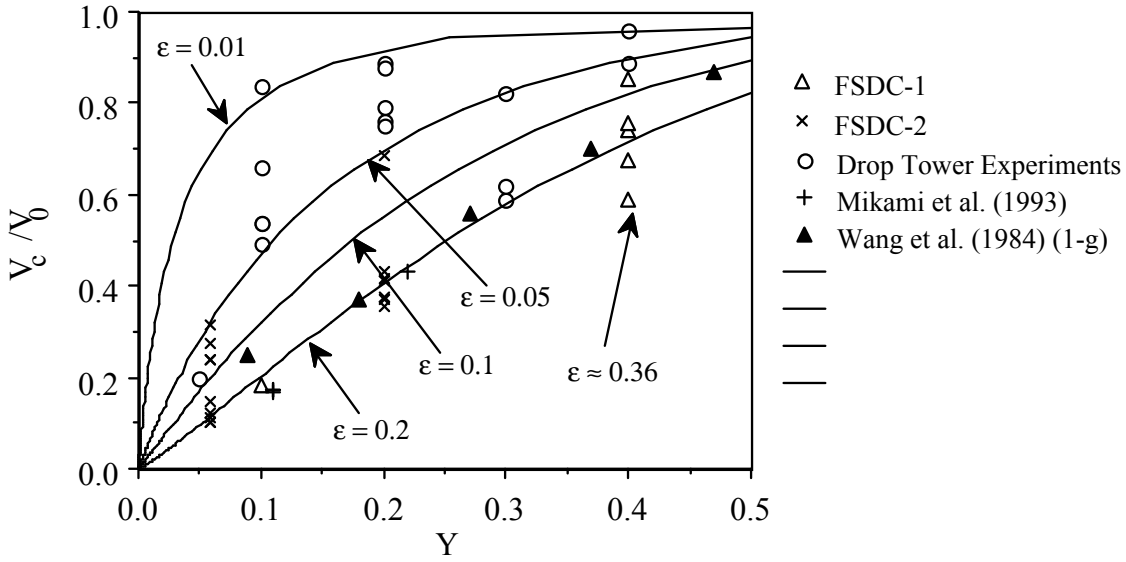

Figure 2: The ratio V_c /V_0 vs. the initial hexadecane mass fraction Y, where V_c is the droplet volume at the onset of flame contraction, and V_0 the initial droplet volume. The lines are theoretical predictions (Aharon and Shaw, 1998) of V_c /V_0 vs. Y for various values of . All experimental data shown, which are for heptane-hexadecane mixture droplets, show the values achieved in the various experiments.

only thermocapillary or solutalcapillary stresses.

In summary, data from well characterized bi-component droplet combustion experiments specifically designed to elucidate the role of liquid-phase internal circulation are not available to date. The primary goal of the flight experiments is to provide benchmark experimental data on bi-component droplet combustion over a wide range of initial conditions that could be used to validate numerical simulations and to develop new theoretical models. The detailed experimental objectives and selection of suitable fuel mixtures are further described in the following sections.

2.3 Surrogate Fuel Droplet Combustion

Aviation fuels like JP8 have poor reproducibility of composition in the manufacturing process. Therefore it is difficult to cross-reference laboratory results from different batches. If a surrogate could be identified which matches one or more measures of the combustion performance of JP8, models for predicting combustion could be more easily developed by doing experiments on the surrogate rather than JP8 directly. The microgravity platform with its reduced buoyant flow and ability to promote spherical droplet flames can assist in developing such blends for this purpose.

The concept of surrogates is not new. As far back as the 1920s surrogate fuels were used to understand the influence of composition on performance of gasoline fuels (Colket et al. (2007)). Over the years, a variety of surrogates have been evaluated. The most elementary is a single component fuel, the relevance of which to a real fuel, is at most to represent single phase heat transfer behavior (Edwards and Maurice (2001)). More realistically, blends of several fuels are necessary to exploit differences among individual constituents to attempt to reproduce a specific metric of the real fuel. Surrogates containing two (Kyne et al. 1999) to over twenty constituents (Hakansson et al. (2001)) have been proposed to model performance of real fuels including liquid fuels (e.g., sprays Smith et al. (1985)) and gaseous fuels (e.g., Cooke et al. (2005)). Interestingly,

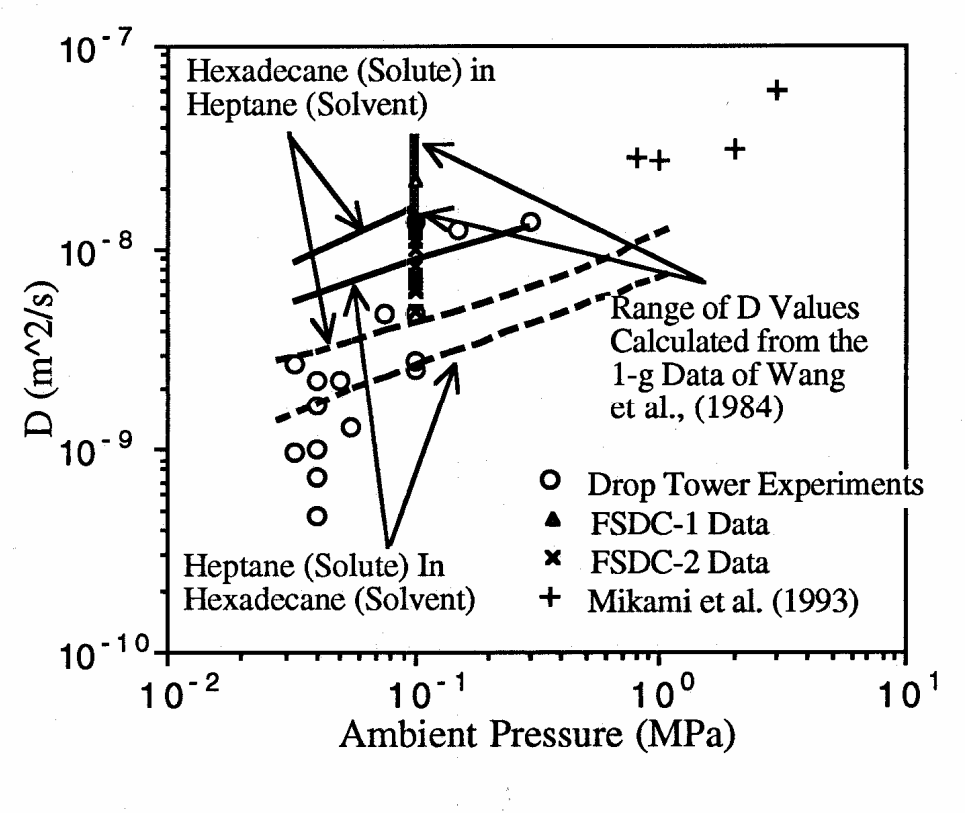

Figure 3: Liquid species diffusion coefficients D (calculated using the relation D = K1/8) as a function of pressure. All data shown are for heptane-hexadecane mixture droplets. The data points are from experiments. The solid lines are D values estimated from correlations (Erkey et al., 1990) using asymptotic predictions of droplet temperatures (Aharon and Shaw, 1998). The dashed lines are D values estimated from correlations (Erkey et al., 1990), where droplet temperatures were assumed to be at the pressure-dependent boiling point of heptane.

Figure 4: a) schematic of a droplet burning with minimal buoyancy; b) backlighted photograph of a 0.52mm nonane droplet showing soot shell (black ring); c) color photograph of a 0.47 mm nonane droplet

Zhang et al. (2007) used the combustion chemistry of heptane as a building block with additional sub-models to predict acetylene concentration in surrogate mixtures of liquid transportation fuels. Smith et al. (1985) proposed a blend of fourteen compounds to match the phase equilibrium and sooting behavior of JP8 in a spray flame.

Recent efforts to develop surrogate fuels have focused on identifying classes of compounds instead of specific fractional amounts. For example, Tsang (2003) noted that the chemistry of real transportation fuels may be described by constituents coming from six chemical classes: iso-paraffins; normal paraffins; single ring aromatics; cyclo-paraffins; olefinic species; multi-ring aromatics. And Colket et al. (2007) identified five chemical classes of transportation fuels (straight-chain alkanes; branched-chain alkanes; cycloalkanes; single-ring aromatics and multi-ring aromatics).

Two aspects that can assist development of surrogate fuels are 1) an appropriate experimental configuration for developing data, and 2) identification of appropriate metrics for the chosen configuration to serve as points of comparison between the surrogate and real fuel. The choice of combustion configuration in which to develop a surrogate should have the following features: 1) transport is easily modelable; 2) the configuration has a capability to produce accurate data; and 3) combustion incorporates some of the unsteadiness associated with liquid fuel burning processes. Several experimental configurations satisfy these constraints for gaseous fuels: counterflow diffusion flame; shock tube; flow reactor; and pool fire to name a few. All have in common that they allow for a numerically tractable configuration from which complex processes, such as soot formation and complex chemistry, can be examined. Regarding liquid fuels, the concept is that the isolated spherically symmetric droplet burning configuration of Fig. 4 belongs among the list of configurations from which surrogates could be developed and which can provide an understanding of the performance of real fuels. For droplet combustion the metrics for comparison include burning rate, burning time, soot aggregate size, extinction diameter, ignition and flame luminosity. Furthermore, unlike the other configurations, the spherical droplet flame configuration experiments proposed here also captures some of the unsteady effects typical of combustion of liquid fuels. No work has thus far been reported on using the spherically symmetric droplet combustion configuration of Fig. 4 for this purpose and the results from this study should provide a unique method for developing a surrogate fuel formula.

2.4 Mechanisms of Soot Formation

Understanding soot formation during the combustion of liquid fuels is important due to its negative effects on the environment and human health as well as for its practical uses in certain industrial processes. Despite its practical relevance the process of soot formation during the combustion of a liquid fuel has not been fully understood due to its complexity (Avedisian (2000)). The process of soot formation involves both chemical and physical aspects: the chemical aspects involve the reaction pathways for the formation of soot precursors, and the physical aspects include nucleation, soot particle surface growth, oxidation, and particle agglomeration. The most widely used models for soot formations include semi-empirical approaches of Moss et al. (Moss et al. (1988); Bressloff et al. (1996)), Lindstedt and co-workers (Leung et al. (1991)), and the detailed models proposed by Frenklach and co-workers (Frenklach and Wang (1991, 1994)).

The earliest observations of sooting during spherically symmetric droplet combustion were those of Okajima and Kumagai (1974b, 1982), Yang et al. (1990), Choi et al. (1990a). More recently Jackson and Avedisian (1994) and Nayagam et al. (1998) measured soot shell diameter for n-heptane droplets. Choi and Lee (1996); Lee et al. (1998) and Chen and Shaw (2000) have obtained soot volume fraction data for droplets of varying initial sizes. The current understanding of sootshell formation suggests that soot particles formed near the flame front are acted upon by viscous drag (caused by Stefan flow), thermophoresis and diffusion. The balance of the various transport mechanisms causes the transient accumulation of soot particles and the formation of a spherical sootshell on the fuel-rich side of the diffusion flame. Further agglomeration of soot within the shell eventually leads to the formation of larger agglomerates that are swept through the diffusion flame by the Stefan drag, and subsequently ignite and burn in the surrounding, hot oxygen rich outer flame zone.

Soot formation during combustion of liquid fuels is inherently linked to the combustion process itself and influence the quasi-steady behavior of droplet burning rate and the transient behavior of flame extinction. There are several suggested mechanisms through which sooting can affect the burning behavior. The formation of soot through pyrolysis reactions (pyrolysis reactions are strongly endothermic) is a heat sink (Choi et al. (1990b);Jackson et al. (1992)). This factor will reduce the effective heat of combustion and therefore the transfer number. Although the transfer number appears in the natural log term of the d^2-law, reduction in the burning rate is expected for conditions of significant soot conversion. Related to this phenomenon is the accumulation of the formed soot in a sootshell. This material contains chemical energy not released in the flame and thus causes a reduction in the effective heat of combustion (Choi et al. (1990b);Jackson et al. (1991)). The magnitude of this effect is related to the soot conversion ratio (mass of soot formed divided by mass of fuel consumed). The presence of soot can also modify the thermophysical properties of the soot-laden gas. The thermal conductivity is higher for soot compared to the surrounding gas, but the overall conductivity of the mixture is not expected to be much different from the gas since contact among soot aggregates to form a solid structural shell is unlikely. The presence of the soot in the fuel-rich region can also affect the radiative emission and reabsorption, thereby influencing the flame temperature distribution.

Since soot is a broad band emitter, its presence between the droplet surface and the flame could influence radiative heat loss from the flame zone. The enhanced soot radiation near flame zone could lead to droplet heat up by liquid phase absorption or an overall reduction in heat transferred back to the droplet caused by reduced flame temperature and absorption of the radiation from the flame by the soot-containing region. When the loss mechanism dominates the flame temperature will be lowered sufficiently and cause radiative extinction of the flame as observed by Nayagam et al. (1998). A comprehensive theoretical or numerical model, which includes soot formation

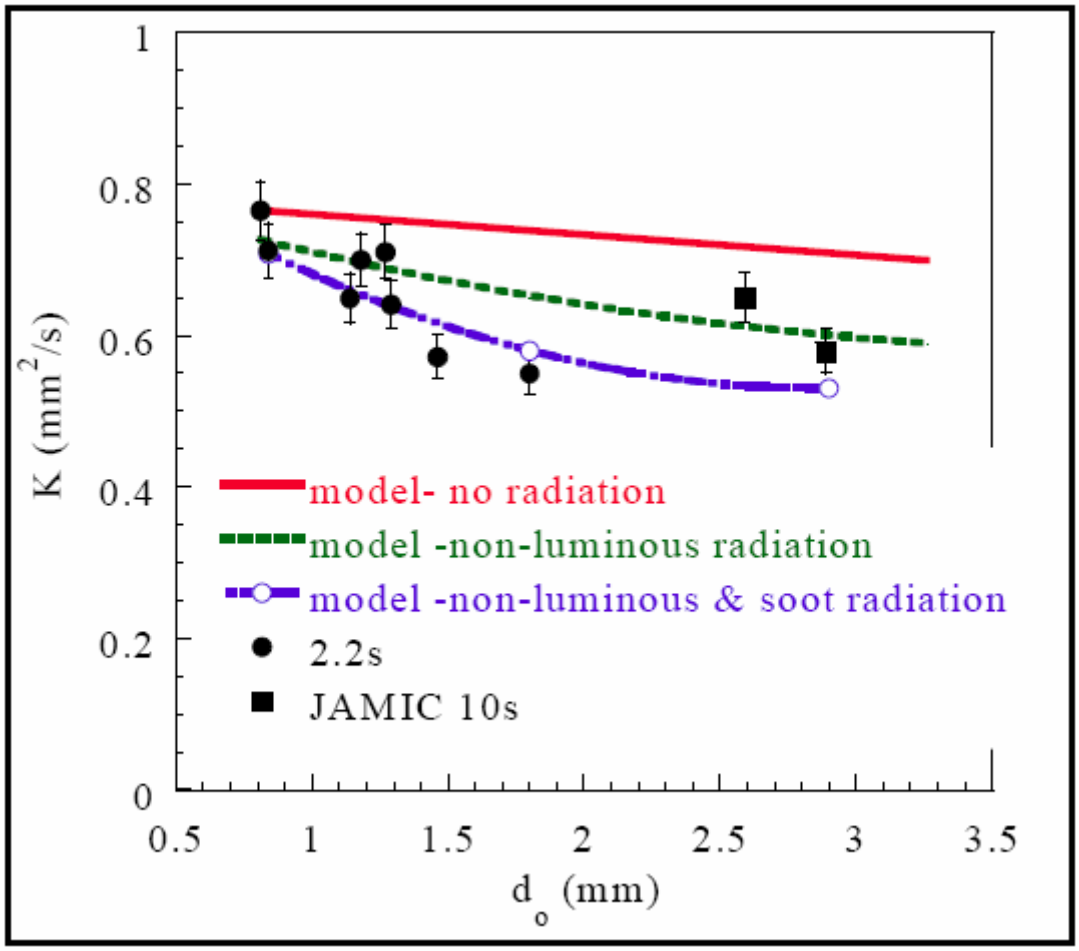

Figure 5: Measured and predicted droplet burning rate as a function of initial droplet diameter. Model predictions were obtained for a)no radiation, b)non-luminous radiation, c)non-luminous and luminous (soot) radiation cases.

process (chemical and physical aspects) and radiation, that can predict radiative extinction is still not available. Manzello et al. (2000) have included the luminous radiation from soot in their numerical calculations by including the measured soot volume fraction values. Figure 5 displays the measured and computed burning rates for various initial droplet diameters. More recently, Kumar et al. (2002) have presented a soot model that includes soot nucleation, growth, and coagulation and O_2 and OH oxidation for transient combustion of spherically symmetric n-heptane droplets.

Understanding soot formation is also important in fire safety applications. Fire sensing technology in microgravity environments typically relies on scattering from particles(Urban et al. (1997)). Characterization of soot morphological properties including the primary particle size, d_p, radius of gyration, R_g, and fractal dimension, D_fr, and their evolution with residence time under various environmental conditions are important for the analysis of soot processes including primary particle growth, soot agglomeration and oxidation processes.

Despite the progress that has been made over the past several decades, systematic detailed measurements of soot properties over a wide range of initial and ambient conditions that could be used to develop and validate theoretical and numerical models are not yet available. The proposed

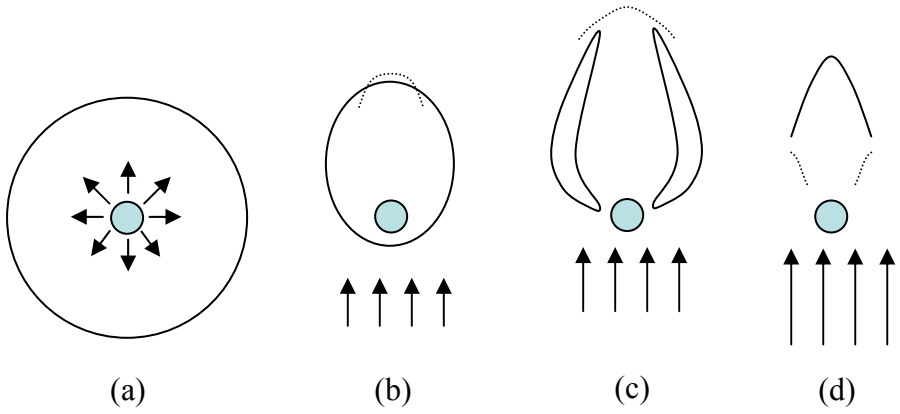

Figure 6: Schematic illustration of various flame configurations.

soot measurements in FLEX-2 investigation should provide some of these data for at least two different fuel types, as described in the following sections.

2.5 Slow Convective Effects

As described in the previous section droplet combustion involves interaction among different time scales, namely residence time, chemical time, radiation time, etc. Often, in many practical applications there exists a relative motion between the droplet and surrounding gas. Forced convective flow imposed on a burning droplet introduces an additional time scale ($\sim d/U_\infty$), where U_∞ is the relative gas/droplet velocity and d is the droplet diameter. This fluid mechanical time scale interacts with other characteristic time scales (e.g., liquid and gas phase diffusion, chemical kinetic) and modifies the results of quiescent droplet combustion for burning rates, flame dynamics, soot and other pollution formation, as well as ignition and extinction conditions. The most visible demonstration of this fact is that when a droplet burns in a convective environment it can support several different flame configurations, namely, an envelope flame, side-boundary-layer flame, and wake flame, unlike the quiescent burning case where only an envelope flame is possible.

Despite both practical and scientific relevance, effects of forced convection on droplet combustion, in particular combustion in a slow convective flow regime where the Reynolds number defined as $Re = dU_\infty/\nu_\infty$ where ν_∞ is the kinematic viscosity of the oxidizer at the ambient temperature is of the order one or less, has received very little attention in the past. Most of the results available thus far rely heavily on semi-empirical approach resulting in correlations of experimental measurements and numerical simulations (Chiu (2000)).

The classical works of Frossling (1938), and Ranz and Marshall (1952) were concerned with the evaporation rates of fuel droplets in a flowing stream. The well-known Frossling Ranz-Marshall (FRM) correlation,

$$Nu = 2.0 K_1 Pr^m Re^n \tag{1}$$

where $Nu = hd/k$ is the Nusselt number, $Pr = \alpha/\nu$ is the Prandtl number, α is the thermal diffusivity, k is the thermal conductivity, h is the heat transfer coefficient, and the exponents m and n are 1/3 and 1/2, respectively, and the constant $K_1 = 0.6$, is originally developed for evaporating droplets. Numerous studies since then have developed several ad-hoc techniques to account for the high gasification rates and the thermophysical property variations during combustion. These semi-empirical correlations include those of Eisenklam et al. (1967), Law and Williams (1972) and Sirignano (1999). The major draw-back of these semi-empirical correlations is that they lack

universal validity and are limited to certain range of conditions. While these approximate analyses provide a useful way to make complex spray calculations, they do not provide concrete physical predictions to test against experimental measurements.

Fairly sophisticated numerical simulations of convective droplet combustion have been developed in the last decade. The key contribution of these numerical models is the inclusion of full Navier-Stokes equations for the gas-phase flow field. However, due to the inherent complexity of the problem, varying degrees of approximations have been made in treating the chemistry, radiation, and the coupling between the gas and liquid phases. Dwyer and Sanders (1986, 1988) have presented unsteady numerical calculations for a single droplet burning in a flowing stream for Reynolds number ranging from 100 initially to small values. Huang and Chen (1998) numerically solved conservation equations for steady burning of a fuel droplet under buoyancy induced flow conditions (normal gravity conditions). More recently Gogos and co-workers Pope and Gogos (2005); Raghavan et al. (2006) have developed a comprehensive numerical code capable of simulating both the liquid-phase and solid-phase processes during droplet combustion in slow convective flows. Their numerical code at this time can not simulate combustion of large droplets or sooting droplets where radiation and soot formation become important.

Theoretical treatments of slow convective droplet combustion stem from the fluid dynamic studies on the motion of a spherical particle in a quiescent environment. In these studies, the convective effect is considered as a perturbation to the spherically symmetric combustion and a suitable small perturbation parameter is identified. The gas-phase conservation equations are then expanded in terms of this small parameter to obtain a perturbation problem to be solved using method of matched asymptotic expansions. Fendell and co-workers (Fendell et al. (1966)) were the first to investigate the effects of forced convection on droplet burning. In their analysis the small perturbation parameter is the Peclet number $Pe(= U_\infty d/D << 1)$. Ayyaswamy and co-workers (Sadhal and Ayyaswamy (1983); Gogos et al. (1986); Gogos and Ayyaswamy (1988); Jog et al. (1996)) removed many of the approximations included in Fendell et al. (1966) and developed a perturbation solution using Reynolds number as a perturbation parameter. Recently Ackerman and WIlliams (2005) developed an asymptotic model for droplet combustion valid for small Reynolds number regime.

Okajima and Kumagai (1974b, 1982) were the first to report experimental results for fuel droplets burning in a slow convective flow. Their experiments were carried out in a microgravity environment (drop-tower) at atmospheric pressures using a wind tunnel. Their limited number of experimental data seemed to follow the FRM correlation with the constant in equation (4) close to 0.3. Gokalp et al. (1988) reported observations of n-heptane droplets burning in a forced convective flow under normal gravity and in microgravity (parabolic flights on board KC-135 aircraft). They observed wake flames for a Reynolds number value of 65 based on ambient properties. Their results also showed that Frossling-type correlations agreed with the forced flow results (with the constant K in equation (4) equal to 0.25) conducted under normal gravity and not with the microgravity experiments. A limited number of convective droplet experiments were conducted using the Glovebox facility in the Spacelab during the USML-2 and MSL-1 space shuttle flights (Dietrich et al. (1996); Nayagam et al. (1998)). Figure 7 shows the effect of forced convection on methanol droplet burning in microgravity.

Bench mark data for convective droplet combustion including burning rates, gas-phase flame dynamics, soot-shell structure and extinction diameters, for sooting and non-sooting fuels under slow convective flows are currently not available. In order to develop a comprehensive theoretical and numerical models for convective droplet combustion detailed measurements over a range of initial conditions are needed.

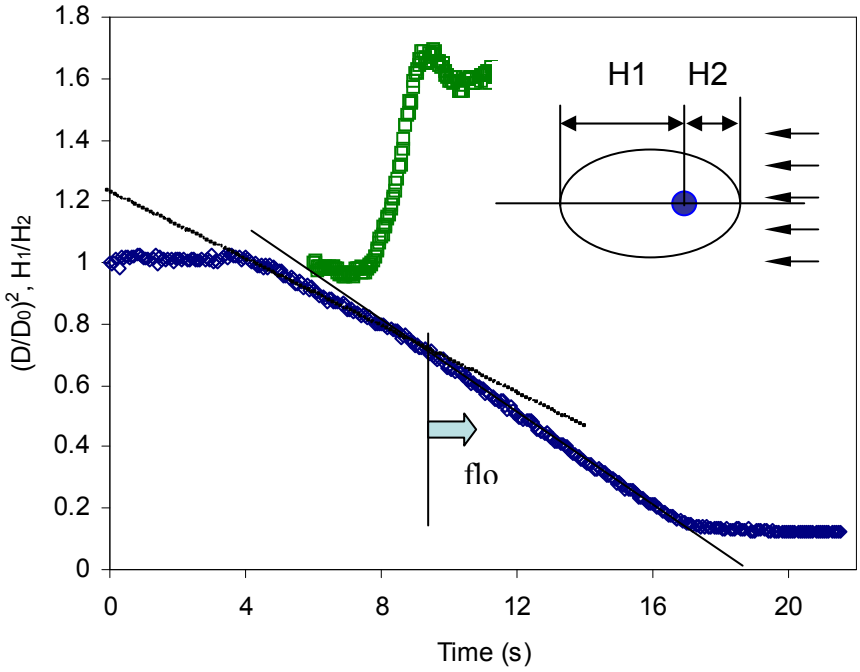

Figure 7: Effect of forced convection on methanol droplet burning in microgravity Dietrich et al. (1996).

2.6 Droplet Arrays Combustion

Studying small numbers of interacting droplets in a well-controlled geometry represents a logical step in extending single droplet investigations to more practical spray configurations. Studies of droplet interactions date back to Rex et al. (1956) , and were most recently summarized by Annamalai and Ryan (1992) and Annamalai (1995). Most studies determined the change in the burning rate constant, K, as a result of interactions. The changes in K occur as a result of two competing mechanisms. The burning droplets compete for the available oxidizer, but there is also a reduction in the heat loss from the flame. Under certain conditions, there exists a separation distance where the droplet lifetime reaches a minimum (Rex et al., 1956; Sangiovanni and Kesten, 1976; Xiong et al., 1984). Additionally, since inter-droplet separation distance, L, increases relative to the droplet size, D, as the burning proceeds, the burning rate is not constant throughout the burn, but changes continuously with time (Miyasaka and Law, 1981; Xiong et al., 1984). These experiments were all in normal gravity, and the strong buoyant flow strongly influenced the observations.

The majority of the experimental studies cited were in terrestrial laboratories. Both Law and co-workers (Miyasaka and Law, 1981; Xiong et al., 1984) and Mikami and co-workers (Mikami et al., 1994), however, did perform their experiments in reduced buoyancy environments produced using reduced pressure conditions. Law and co-workers utilized low pressure, high oxygen ambients, and Mikami and co-workers used drop towers. The oxidizer concentration in the ambient had to be high ($> 40\%$) in Lawś studies, however, to avoid extinction or ignition limits due to the reduced pressure. Both of these studies concluded that interactions retarded droplet heating early in the droplet lifetime. Mikami and co-workers further found that the burn time of an array reached a minimum at a critical inter-droplet spacing. They assert that this minimum results from the opposite effects of radiative enhanced heating of the droplets and competition for the available oxygen. While both diffusive and radiative extinction of single droplets in microgravity have been

observed before (Dietrich et al. (1996); Nayagam et al. (1998), there exists almost no information on how droplet interactions affect the extinction limits.

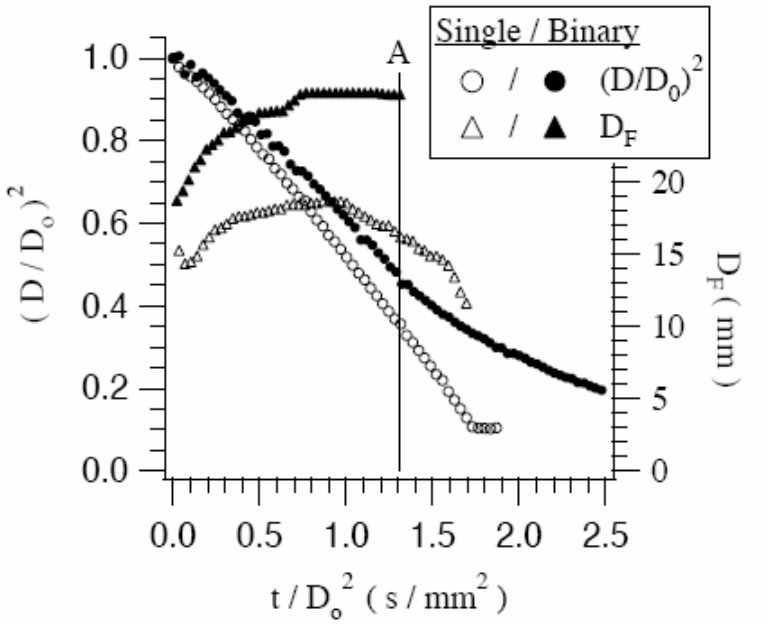

Figure 8: Normalized droplet diameter squared and flame height for a single droplet and binary droplet array (L = 3.3 mm) burning in an ambient oxygen mole fraction of 0.15 (balance nitrogen) at 190 mmHg total pressure in microgravity

Figure 8 shows the burning behavior for a single droplet and a binary array ($L \approx 3\,mm$) in a 0.15 oxygen mole fraction (balance nitrogen), 190 $mmHg$ ambient. There are several noteworthy features of the single droplet burning behavior. First, this ambient condition was not flammable in normal gravity. In fact, in this ambient oxygen mole fraction, droplets of this size could not sustain a flame in normal gravity at pressures up to 760 $mmHg$. Figure 8 also shows that while the single droplet burned to completion, the flame surrounding the array extinguished approximately one second after the igniter withdrew. The droplet diameter at flame extinction was approximately 1.1 mm for both droplets of the array. Further, the flame size was nearly 50 percent larger than the flame surrounding the single droplet and the flame was much dimmer (evaluated by the intensity of the video images). In the binary array test, the flame size increased, reached a maximum, and extinguished. The above trends were consistent over a range of inter-droplet spacings and ambient pressures. In the 0.15 oxygen mole fraction ambient, the flame surrounding the binary array always extinguished at a finite droplet size that was larger than the single droplet extinction diameter.

Figure 9 shows a similar results for a single and binary droplet array burning in oxygen/helium environment. The burning rate constant K was much higher for the helium diluted experiments than those in the nitrogen diluted experiments (Fig. 8). Also, the flames were much brighter in the He/O_2 ambients and the flame sizes and standoff distances in the He/O_2 ambients were approximately 50 percent smaller. The flame surrounding the single droplet extinguishes quickly after ignition ($D_{ext} \approx 1.4\,mm$). The flame surrounding the binary array, however, burns much longer, and the extinction droplet diameter is much smaller ($D_{ext} \approx 1.1\,mm$). This extinction trend is opposite to that displayed in O_2/N_2 experiments, but in agreement with the normal gravity experiments. The K for the binary array (0.75 mm^2/s) was smaller than K for the single droplet (0.90 mm^2/s), although there is only a short time period in the single droplet experiment to

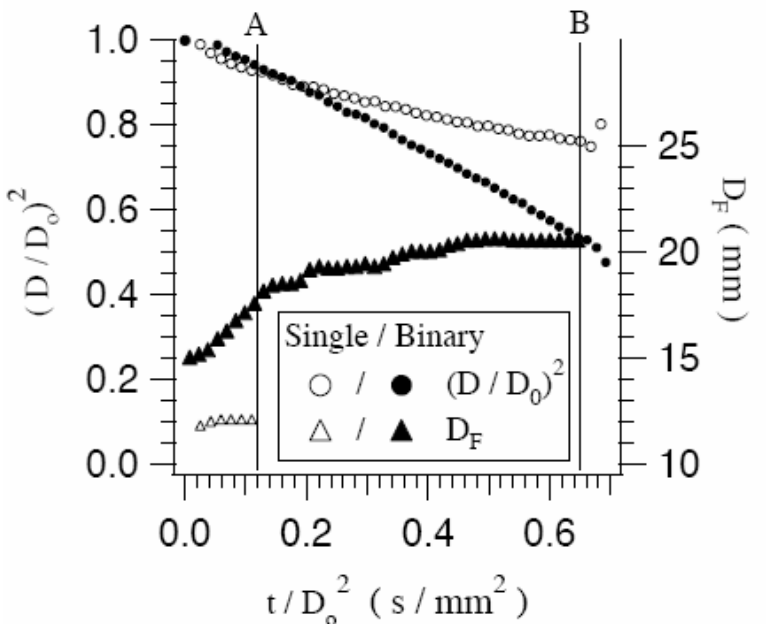

Figure 9: Normalized droplet diameter squared and flame height as a function of normalized time for a single droplet and binary droplet array ($L = 3.7\,mm$) burning in an ambient oxygen mole fraction of 0.25 (balance helium) at 190 $mmHg$ total pressure in microgravity

calculate K. The flame height for the binary array was larger than the flame height for the single droplet. Further tests showed that the flames surrounding the binary droplet array at inter-droplet spacings of $L \approx 8$ and 12 mm (merged flames existed for both spacings) both extinguished at droplet diameters smaller than the single droplet. The extinction behavior at an inter-droplet spacing of 24 mm, however, was nearly identical to that of a single droplet.

The helium and nitrogen-diluted microgravity experiments clearly exhibit different extinction behavior for the binary arrays versus the single droplets. The single droplets and binary arrays in the nitrogen ambient have very large, weak flames and small burning rate constants (relative to the helium-diluted tests). Consequently, the ratio of the radiative heat loss from the flame zone to the energy release from combustion is likely much larger for the nitrogen-diluted tests. This ratio increases with droplet size since the radiative loss increases with the cube of the droplet diameter while the heat release increases proportionally to the droplet diameter (assuming K is independent of droplet diameter). Therefore one could speculate that the increase in flame size, and decrease in K from the single droplet to the binary droplet array increases the ratio of radiative loss to energy release, potentially enough to cause extinction of the binary array. Alternately, if the inter-droplet spacing were to approach zero for a binary droplet array, this would create a single droplet whose size is 26 percent larger than each individual droplet. This increase in droplet size and corresponding increase in radiative loss relative to heat release could be enough to cause extinction of the flame surrounding the binary array. A similar argument can be made to explain the behavior of the helium-diluted tests. The decrease in flame size, increase in K, and the results of previous work Nayagam et al. (1998) lead us to believe that the helium-diluted experiments were less dominated by radiative loss. Since radiative loss is not dominant, the flame temperature is (approximately) independent of the flame size (Williams, 1985). Extinction occurs when the residence time is smaller than the required chemical reaction time, the later of which is independent of droplet diameter in this regime (diffusive extinction). For the binary droplet array, if the inter-droplet spacing were

zero, this would again create a larger single droplet, with a correspondingly larger flame. This single droplet would have a larger residence time, and the flame would not extinguish until the droplet size was equal to the single droplet extinction size. The data in Fig 9 support this view. If the two droplets in the array at flame extinction merged, the resulting single droplet would have a droplet size very close to the extinction droplet size in the single droplet test. Almost no theoretical or numerical studies exist to compare with the present experiments.

3 Research Goals

3.1 Liquid-Phase Phenomena

As described in the previous section the overall objective of the bi-component droplet combustion experiments is to examine the role of liquid phase mixing on the burning characteristics of a single droplet. Liquid phase mixing caused either by thermocapillary flows or by solutalcapillary flows will be investigated.

The experiments will examine the burning behavior of single droplets over a range of the parameter ε. This is accomplished by examining different fuel mixtures, ambient pressures, oxygen mole fractions, and also altering the time from deployment to ignition (altering the initial liquid motion in the droplet). The flight experiments will involve two different classes of bi-component fuel mixture droplets. The first class is expected from theoretical predictions to be hydrodynamically stable in the sense that droplet internal flows will be damped as a result of stabilizing thermocapillary effects. Alkane fuel mixtures, e.g., heptane and hexadecane, are candidate fuels for these experiments. The heptane-hexadecane droplets will display flame contractions. In addition, differences in surface tension between heptane and hexadecane are small enough such that solutalcapillary effects should be subdominant and these droplets should be hydrodynamically stable. For these droplets, thermocapillary effects should damp internal droplet flows, as suggested by Aharon and Shaw (1996).

The second class of fuel mixture droplets is expected to be hydrodynamically unstable in that droplet internal flows will be strongly promoted as a result of destabilizing solutal-capillary effects that are expected to cause rapid motions in the liquid phase, causing significant mixing within droplets. Candidate fuels for these experiments are 1-propanol and glycerol, which will not absorb significant amounts of water. The propanol-glycerol droplets will display flame contractions as well. However, the surface tension for propanol is much smaller than for glycerol, which should induce hydrodynamic instabilities, i.e., capillary flows from solutalcapillary effects, as suggested by the theory of Aharon and Shaw (1996). In addition, these droplets may absorb small amounts of water from the ambient during combustion - this water will also induce solutalcapillary instabilities. Any absorbed water will be completely miscible with the propanol-glycerol droplet mixture. Complete miscibility is important to allow comparison with present theory.

The ambient pressure changes the boiling temperature of the fuel. The burning rate constant, however, is only a weak function of the pressure. Therefore, by changing the pressure, one can change the ratio of the liquid phase diffusion coefficient to the burning rate constant (the small parameter, ε, in the analyses of Shaw and Williams (1990) and Aharon and Shaw (1998). Estimates indicate that the change in pressure from 1 to 3 atm will result in about a factor of 5 increase in ε. Changes in the ambient composition will cause changes in burning rates by about 50%. In addition, varying the levels of internal circulation within droplets will change effective liquid diffusivities by at least a factor of 2. All of these factors will be allowed to vary by more than an order of magnitude (e.g., from 0.01 to 0.5).

3.2 Surrogate Fuel Droplet Combustion

This area of study involves application of the one-dimensional droplet flame configuration shown in Fig.4 to evaluate the combustion process of hydrocarbons considered as surrogate components of a real transportation fuel such as JP8. The idea is that the spherical droplet flame configuration should be as useful for developing surrogate liquid fuels as counterflow flames, shock tubes, pool fires, stirred reactors, and flow reactors have been to evaluate performance of gaseous fuels. Each of these configurations provides a unique perspective to combustion by targeting specific aspects

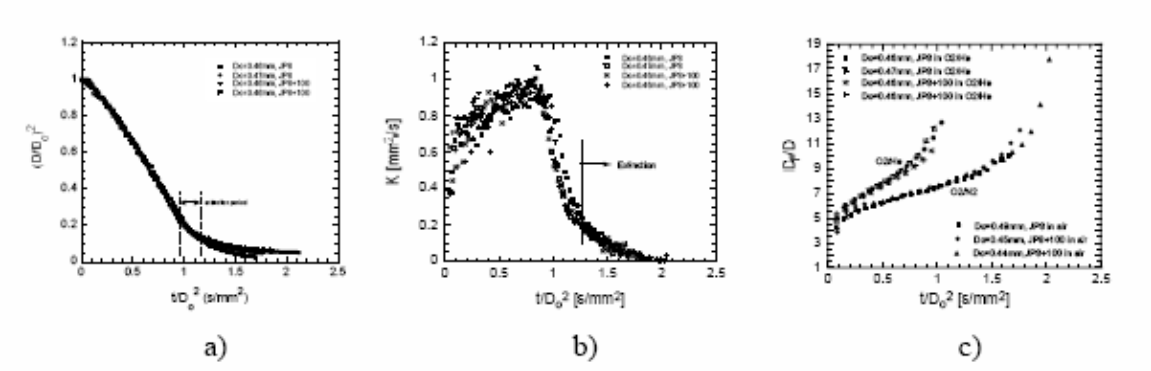

Figure 10: a) JP8 in a 70%He/30%O2 gas; b) burning rate obtained as slope of data in figure c); flame diameter for oxygen with nitrogen or helium.

of the burning process, for example combustion chemistry, ignition and extinction. Furthermore, unlike these other combustion configurations, the spherical droplet flame is important because it captures some of the unsteadiness which is typical of combustion of liquid fuels (i.e., sprays)

Several considerations guide the selection of the liquids for this study. They concern the chemical and physical characteristics of JP8 which is comprised of the following general hydrocarbon classifications: straight chain alkanes, aromatics, branched-chain alkanes, and single ring aromatics (Edwards and Maurice (2001). The liquids are selected for this phase of the ground-based experiments (see, Appendix), are summarized in Table 1.

Table 1: Selected Properties of Fuels.

Name	Formula	T_b(k)	T_c(K)	P_c(atm)	ρ,293K
heptane	C_7H_{16}	372	540	27	680
decane	$C_{10}H_{22}$	447	618	21	730
iso-octane	C_8H_{18}	372	544	26	690
propyl-benzene	C_9H_{12}	432	638	32	860
hexanol	$C_6H_{14}O$	430	611	41	820
JP8	$C_{11}H_{21}$	395-473	576	23	810

The boiling point ranges of the liquids in Table 1 are close enough that microexplosions should not be expected to occur for blends of the liquids. This is an important consideration because of the droplet deployment design which will be used in the proposed experiments. Three mixtures are also included in the study: heptane/octane mixture (which has long been considered as a surrogate for gasoline since the 1920s); decane/propylbenzne (currently under consideration in Europe as a surrogate (Colket et al. (2007)) and JP8/hexanol. Hexanol is included because of its significantly reduced sooting propensity while also having a boiling point in the range of the other liquids listed in Table 1. With the exception of hexanol, all of the hydrocarbons soot extensively. We expect soot shells to form and for soot shell diameter to be included in the database to be developed as part of the proposed research except possibly for JP8. One of the purposes of hexanol will be to reduce soot formation through blending to allow observation of the droplet through a dense soot cloud. This problem will be an important consideration for JP8 which soots so extensively that the droplet cannot easily be observed through the soot cloud (Bae and Avedisian (2005, 2004)).

The initial droplet diameters will be in the sub-millimeter range for the ground-based investi-

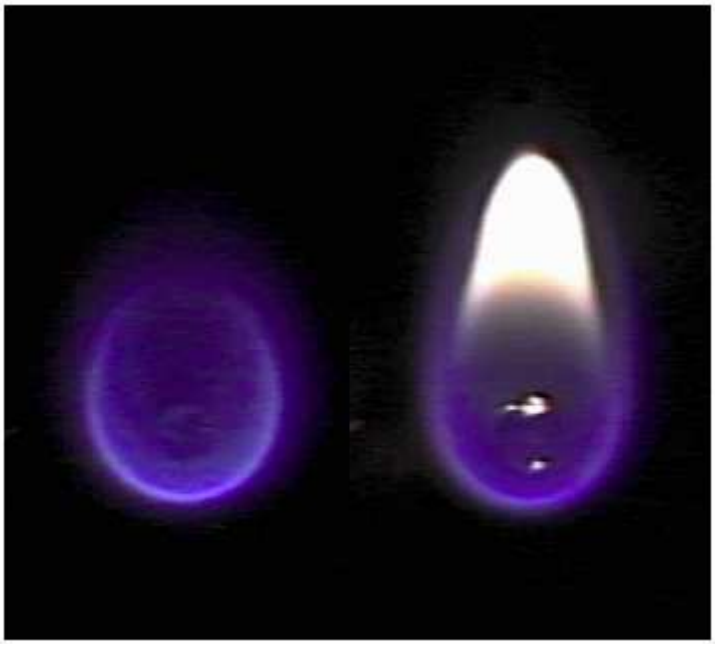

Figure 11: Burning of ethanol droplet in normal-gravity under 1 and 2 atmospheric pressures.

gations. The information from droplets of this size will bridge to larger droplet studies pursued in the FLEX-2 flight experiments. There are a number of aspects of the burning which are droplet-size-dependent, most notably the evolution of droplet diameter and the droplet burning rate, and soot formation (Lee et al. (1998); Jackson et al. (1992); Jackson and Avedisian (1994)), which will benefit from comparisons between large and small droplet results. The ambient will include inerts of nitrogen (e.g., air) and helium or CO2. An ambience of He/O2 in particular is effective in controlling sooting of JP8 droplets (Bae and Avedisian (2004)), which also shows evidence of flame extinction. Measurements will be made of the following: evolution of droplet diameter (if soot does not obscure the droplet visibility) and flame structure, burning rate (slope of D^2), burning time, extinction diameter (if extinction occurs), and soot shell diameter. Examples of some representative data for JP8 using equipment similar to that of MDCA apparatus are shown in Figure 10 (Bae and Avedisian (2004)). Specific experimental objectives are described in the following sections.

3.3 Sooting Effects

The primary fuels that are being considered in the FLEX-2 program are known to display significant sooting behaviors. Previous studies indicate that sooting behavior can influence droplet burning rate, flame temperature, flame radiative emission, and extinction behavior. The overall objectives of the sooting effects study is to obtain quantitative data (soot volume fraction and soot temperature) from a heavily-sooting alkane fuel and an variably-sooting alcohol fuel so that detailed models can be developed and validated for soot processes that affect quasi-steady and transient droplet burning behaviors. Furthermore, the measurements of soot volume fraction and soot temperature may provide important insights for sub-mechanisms that will affect droplet burning rate, flame temperatures, radiative emission, and flame extinction for the related studies on slow-convection, droplet arrays, surrogate fuels, and liquid-phase phenomena.

3.4 Slow Convective Effects

Convective droplet combustion is inherently a complex problem involving nonlinear interactions among disparate time and length scales. Review of the literature clearly reveals that most of the work in this area has been motivated primarily by spray combustion applications and rely heavily on empirical or semi-empirical methods using limited experimental data and numerical simulations. Fundamental physical processes, especially those involving transient phenomena are still not well understood. Experiments involving controlled transient effects including droplet acceleration/deceleration and extinction are scarce if not nonexistent. In the low Reynolds number regime, with envelope flames, there are a limited number of microgravity experimental data obtained in air at atmospheric pressures. In order to develop comprehensive theoretical models and validate them, more systematic experimentation over wider range of parameters is needed (Avedisian (2000)).

In the modeling arena both numerical simulations and theoretical models which use asymptotic techniques are available for convective droplet combustion. However, these models include a variety of simplifying assumptions and are in need of more comprehensive comparisons against experiments. Transient phenomena including extinction and acceleration/deceleration effects have scarcely been addressed in the past. The present project is aimed at obtaining systematic data on convective droplet combustion in the small Reynolds number regime over a range of droplet and environmental conditions and should help in the development of comprehensive theoretical models. Specific objectives of the slow convective droplet combustion study are described in the next section.

3.5 Droplet Arrays Combustion

The droplet arrays experiments described in the previous section provided unique insight into the extinction behavior of droplet arrays compared to single droplets. The data, however, were limited by the time available in the microgravity facilities. Ideally, there would be sufficient test time to observe both radiative and diffusive extinction in a single test ambient (nitrogen or helium). Ground-based microgravity facilities do not have sufficient reduced gravity time (drop towers) or quality (aircraft) to get data over a range of droplet sizes and ambient environments. The proposed experiment will examine the burning behavior of binary droplet arrays over a range of droplet sizes, droplet separation distances and ambient environments where it is possible to observe both diffusive and radiative extinction. The goal of the work is to test determine the flammability map of both the single droplet and droplet array and determine how droplet interactions influence the extinction and flammability limits.

Figure 12 shows a conceptual flammability diagram of a single droplet and a binary droplet array. The abscissa is the droplet size and the ordinate is the ambient oxygen mole fraction. For the single droplet the left branch represents the diffusive extinction regime and the right branch represents the radiative extinction regime. Inside this boundary quasi-steady burning is possible, and outside it is not. In a typical droplet combustion experiment ignition occurs at a point inside the boundary, and burning proceeds along a horizontal line up until the diffusive extinction boundary line, where the flame extinguishes. The results presented in the previous section suggest that droplet interactions shift this boundary to the left as Fig 12 shows. Details of the experimental procedure and specific experimental objectives are described in the following sections.

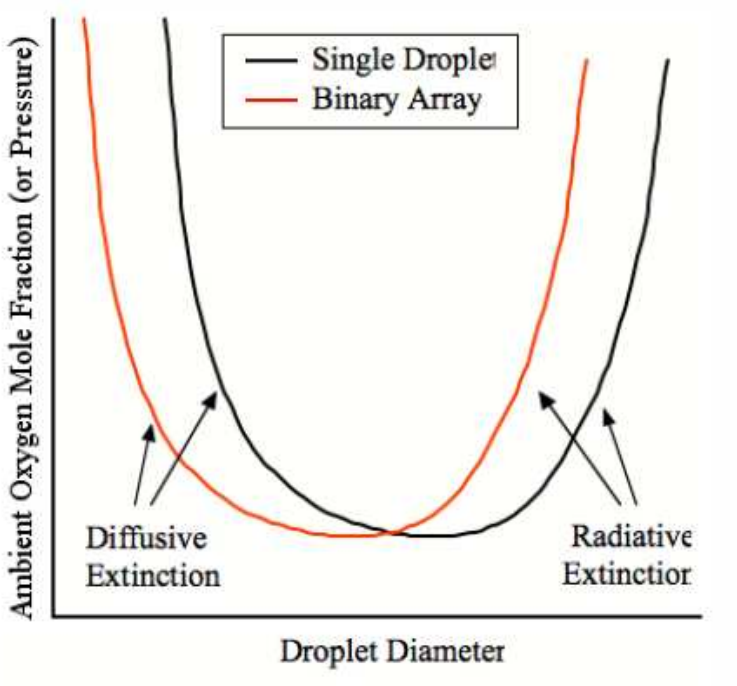

Figure 12: Qualitative representation of the effect of droplet interactions on flammability limits

4 Flight Experiment Description

The flight experiment utilizes the Multiple Droplet Combustion Apparatus (MDCA) installed in the Combustion Integrated Rack (CIR) in the International Space Station (ISS) to investigate several fundamental aspects of droplet combustion. Combustion of large droplets with burning times of the order of tens of seconds are the focus of the flight experiments while the ground-based microgravity experiments are focussed on smaller droplets. From experimental point of view the overall investigation can be grouped into the following four categories, namely

- Pure fuel experiments
- Fuel mixture experiments
- Convective effects experiments
- Droplet arrays experiment

The independently varied experimental parameters during FLEX-2 experiments are: 1) Fuel type, 2)Ambient gas composition, 3)Ambient Pressure, 4)Droplet initial diameter, 5)Droplet translation velocity (and acceleration) and 6)Droplet spacing and initial size in a binary linear array. This section outlines the specific scientific objectives, the diagnostic requirements, and the science data end products for each of the four categories.

4.1 Experiment Objectives

Pure Fuel Experiments: The objectives of the pure fuel studies are to examine the steady and unsteady liquid and gas-phase phenomena, flame extinction, soot formation mechanisms and radiative heat transfer. As explained in the earlier sections, decane ($C_{10}H_{22}$) and ethanol (C_2H_5OH) fuels

are chosen so that we can build on the results of our earlier flight experiments (DCE, FSDC-1 and FSDC-2) with heptane and methanol. In these experiments droplet burning rate, flame dimensions, radiative emissions, and soot volume fraction are measured as a function of time and droplet initial size at different ambient conditions. When flame extinction occurs, the diameter of the unburned droplet at extinction is also determined. The specific set of objectives for these experiments are as follows:

4.1.1 Determine diffusive and radiative flame extinction boundaries for ethanol and decane droplets in test atmospheres containing N_2 or He at pressures ranging from 0.5 atm to 2.5 atm.

4.1.2 Measure droplet extinction diameters for ethanol and decane fuels for validation of detailed and reduced chemical kinetic models.

4.1.3 Measure soot volume fractions and soot temperatures for a range of initial conditions to determine influence on droplet burning and flame extinction.

4.1.4 Measure radiant emissions from both luminous and non-luminous flames in test atmospheres containing N_2 or He and at pressures ranging from 0.5 atm to 2.5 atm.

Fuel Mixture Experiments: Bi-component fuel mixtures are chosen to examine the role of liquid phase transport effects as well as to study the burning characteristics of simulated 'real' fuels. Propanol/glycerol and heptane/hexadecane mixtures are used to examine the role of liquid phase diffusion, preferential evaporation, and mixing in the burning characteristics of fuel mixtures. Heptane/octane and decane/propylbenzene experiments are focussed on simulating the characteristics of 'real' fuels, like gasoline and jet fuels, which contain a variety of hydrocarbon with differing volatilities. The experimental measurements made during these experiments are similar to the pure fuel studies, however, the initial fuel composition and the interpretation of the results are different. The primary objectives of these experiments are as follows:

4.1.5 Measure diameter d_c at the onset of flame contraction relative to the initial droplet diameter d_0. Correlate with theoretical predictions and provide estimates for effective liquid diffusivities.

4.1.6 Measure burning rate, burning time, extinction diameter, and flame luminosity for the JP8 surrogate fuel mixtures.

Convective Droplet Experiments: The overall objectives of this set of experiment are to investigate the effects of slow convective flows on the burning characteristics of liquid-fuel droplets. The imposed flow velocities are such that the Reynolds number based on initial droplet diameter is of the order unity. The specific objectives of the present flight experiments are as follows:

4.1.7 Obtain radiative and diffusive flame extinction limits in the low Reynolds number flow regime over the range of ambient test pressures and oxygen concentrations.

4.1.8 Measure droplet regression rates for sooting (decane) and non sooting (ethanol) fuels as a function of imposed flow at low velocities over a range of ambient oxygen concentrations and pressures.

4.1.9 Measure flame stand-off distance, flame shape, and temperature field measurements in low flow velocities under a range of test atmospheres for use in validation of detailed theoretical models (i.e., radiative and finite-rate chemical kinetic effects).

Droplet Arrays Experiments: The objectives of the droplet arrays experiments are to investigate the droplet-droplet interactions on the diffusive and radiative extinction of the flame surround the droplets for various L/D_0 ratios using pure fuels. The specific microgravity experimental objectives are as follows:

4.1.10 Determine the flammability map (diffusive and radiative extinction limits) for a binary droplet array as function of L/D_0 ratio.

4.1.11 Measure variations in burning rate constant k as a function of L/D_0 for a range of ambient conditions to verify theoretical predictions.

The overall FLEX-2 experiments consist of a series of droplet combustion experiments to examine the fundamental aspects of pure and fuel-mixture droplets. The experiments involve dispensing, deploying and igniting a single droplet in a known and controlled gaseous environment. The ignited droplets burns to either completion or the flame extinguishes at a finite droplet radius in a quiescent ambient. During the droplet arrays experiments, two droplets are placed along a support fiber at known locations and the droplets are ignited simultaneously and the subsequent burning is recorded. In the convective flow tests the droplet is subjected to a known and controlled small, sub-buoyant flow. The primary independent experiment variables are described in the next section followed by a discussion of the diagnostics. The exact requirements in tabular form for the hardware and diagnostics are discussed in subsequent sections.

4.2 Test Matrix Envelope

The test matrix envelope is chosen so that all the science objectives stated earlier can be met within the MDCA hardware constraints. Detailed experimental test points are not provided at this time. However, on-going ground tests in the drop towers, experimental results from FLEX-1 (e.g., this experiments predecessor experiment), as well as numerical and theoretical analyses will be used to define a detailed test matrix as the program evolves. To help estimate resource requirements for

Table 2: FLEX-2 Test Matrix Envelope

Experiment Variable	
Pure Fuels	decane, ethanol
Fuel Mixtures	heptane/hexadecane mixtures
	propanol/glycerol mixtures
	heptane/octane
	decane/propylbenzene
Ambient Gas	O_2/N_2 mixtures
	O_2/He mixtures
Oxygen mole fraction	0.17, 0.21, 0.25, and 0.30
Ambient Pressure	0.5, 1.0, 1.5, 2.0, and 2.5 atm.
Initial Droplet Size	1.5 to 5.0 mm
Arrays Configuration	binary linear
Flow Velocity	0.1 to 5 cm/s

the flight program we provide the following estimates for the number of tests for each investigation. Conservatively an average initial droplet diameter of 3 mm can be assumed for all the tests. The bi-component fuel mixtures can be assumed to be a 50-50 mix of each component for resource estimation, though different mixtures composition will be specified at a later date.

Table 3: Estimated Number of Tests

Experiment Category	Fuel	No. of Tests
Pure Fuel (quiescent)	decane	100
	ethanol	100
Pure Fuel (flow)	decane	50
	ethanol	50
Pure fuel (arrays-2)	ethanol	25
(arrays-2)	decane	25
Fuel Mixture	heptane/hexadecane	50
	propanol/glycerol	50
	heptane/octane	50
	decane/propylbenzene	50

4.3 Science Data End Products

The Science Data End Products represent the manner in which the data obtained from testing will be analyzed and ultimately presented. This information is presented in Table 4.3 on the following page and provides a summary of the diagnostics necessary to meet the stated science objectives.

Table 4: Science Data End Products.

No.	**Science Objectives**	**Diagnostics**	**Science Data End Product**
		Pure Fuel Tests	
4.1.1	Determine diffusive and radiative flame extinction boundaries for ethanol and decane droplets in test atmospheres containing N_2 or He at pressures ranging from 0.5 atm to 2.5 atm	- OH flame view with CIR LLL-UV camera - Flame view with MDCA color camera - Back-lit images from CIR HiBMs cameras	- droplet and flame histories with pre-ignition, ignition, extinction and post-extinction behavior
4.1.2	Measure droplet extinction diameters for ethanol and decane fuels for validation of detailed and reduced chemical kinetic models.	- OH flame view with CIR LLL-UV camera - Flame view with MDCA color camera - Back-lit droplet images from CIR HiBMs cameras	- plots of D_{ext} as a function of oxygen concentration and pressure for ethanol and decane

4.1.3	Measure soot volume fractions and soot temperatures for a range of initial conditions to determine influence on droplet burning and flame extinction	- CIR HiBMs w/ LCTF - OH flame view with CIR LLL-UV camera - Back-lit droplet images from CIR HiBMs cameras	- plots of burning rates and droplet extinction diameters as a function of SVF - plots of SVF as a function of pressure and oxygen concentrations
4.1.4	Measure radiant emissions from both luminous and non-luminous flames in test atmospheres containing N_2 or He and at pressures ranging from 0.5 atm to 2.5 atm	- OH flame view with CIR LLL-UV camera. - flame view with MDCA color camera. - OH flame view with CIR LLL-UV camera - wide and narrow band radiometers	- plots of narrow-band and broad-band emissions as a function of time for different ambient conditions
		Fuel Mixture Tests	
4.1.5	Measure diameter d_c at the onset of flame contraction relative to the initial droplet diameter d_0	- OH flame view with CIR LLL-UV camera. - flame view with MDCA color camera - OH flame view with CIR LLL-UV camera - back-lit images from CIR HiBMs cameras	- plots of d_c for different ambient conditions and fuel mixtures
4.1.6	Measure burning rate, burning time, extinction diameter, and flame luminosity for the JP8 surrogate fuel mixtures.	- OH flame view with CIR LLL-UV camera. - flame view with MDCA color camera - OH flame view with CIR LLL-UV camera - back-lit images from CIR HiBMs cameras	- plots of d^2 versus time for different ambient conditions and fuel mixtures
		Slow Convective Tests	

4.1.7	Obtain radiative and diffusive flame extinction limits in the low Reynolds number flow regime over the range of ambient test pressures and oxygen concentrations	- back-lit droplet images from CIR HiBMs cameras - OH flame view with CIR LLL-UV - wide and narrow band radiometers	- plot of extinction diameter as function of Reynolds number for various ambient conditions - dimensionless plots of extinction Damköhler number versus Reynolds number
4.1.8	Measure droplet regression rates for sooting (decane) and non sooting (ethanol) fuels as a function of imposed flow at low velocities over a range of ambient oxygen concentrations and pressures	- back-lit droplet images from CIR HiBMs cameras - OH flame view with CIR LLL-UV	- plot of extinction diameter as function of Reynolds number for various ambient conditions - dimensionless plots of extinction Damköhler number versus Reynolds number
4.1.9	Measure flame stand-off distance, flame shape, and temperature field measurements in low flow velocities under a range of test atmospheres for use in validation of detailed theoretical models (i.e., radiative and finite-rate chemical kinetic effects)	- back-lit droplet images from CIR HiBMs cameras - OH flame view with CIR LLL-UV - flame view with MDCA color camera - wide and narrow band radiometers	- plots of flame stand-off, flame height, and flame length as a function of Reynolds number for various ambient conditions
	Droplet Array Tests		
4.1.10	Determine the flammability map (diffusive and radiative extinction limits) for a binary droplet array as function of L/D_0 ratio	- back-lit droplet images from CIR HiBMs cameras - OH flame view with CIR LLL-UV - wide and narrow band radiometers	- plot of extinction diameter as function of Reynolds number for various ambient conditions - dimensionless plots of extinction Damköhler number versus Reynolds number
4.1.11	Measure variations in burning rate constant k as a function of L/D_0 for a range of ambient conditions to verify theoretical predictions	- back-lit droplet images from CIR HiBMs cameras - OH flame view with CIR LLL-UV	- plots of D_{ext} as a function of oxygen concentration and pressure for ethanol and decane - plots of burning rates as a function of L/D_0 for various test conditions

5 Flight Experiment Requirements

5.1 Experiment Requirements

This section describes the experimental requirements and the rationale behind the requirements. A summary of all the requirements is provided in tabular form first, followed by a more detailed explanation about the rationale behind the requirement.

Table 5: Hardware requirements tabulation.

Section	Description	Requirements
5.1.1	Test Fuels	- pure fuel tests: decane ($C_{10}H_{22}$ sooting); ethanol (~~C_2OH~~ non-sooting) - mixed fuel tests: heptane/hexadecane, propanol/glycerol, heptane/octane, or decane/propylbenzene - research grade, dry, degassed, purity greater than 99.5% - fuel temperature at the start of the test shall be in the range of 18 $^oC - 27\ ^oC$
5.1.2	Droplet Deployment and Ignition	- 1.5 mm to 5 mm $\pm$ 0.25 mm and reproducible to within $\pm$ 5% - support fiber diameter $<$ 100 μm and capable of anchoring droplet at a fixed location - hotwire ignition using minimum ignition energy following cessation of deployment-induced oscillations - igniter positioning shall be within 1-5 D_0 away from surface, command controllable to within 0.5 mm, and removable from the field of view - igniter power and duration of powered cycle shall be command controllable to provide ignition of droplet using the minimum ignition energy - for quiescent tests: a spherical *zone-of-exclusion* at least 10 D_0 from droplet center - for non-quiescent tests: cylindrical *zone-of-exclusion* of length 20 D_0 downstream, at least 8 D_0 upstream, and a diameter of 10 D_0 with the center located at the deployment site must be maintained free of any objects, where D_0 is the initial droplet diameter - capability of igniting within a flow field

5.1.3	Initial Pressure	- test pressures at 0.5, 1.0, 2.0 and 3.0 atm ± 0.05 atm - chamber pressure to be maintained within ± 10% of initial pressure throughout each test.
5.1.4	Initial Ambient	- mole fractions of O_2 from 0.10 to 0.40 - diluents will be either N_2 or He - initial gas temperature at 18 $^oC - 27$ ^oC - humidity $<$ 10% for all test points - quiescent atmosphere prior to ignition - well-mixed gases prior to ignition.
5.1.5	Ambient Flow Conditions	- target flow velocities between 0.1 cm/sec and 5.0 cm/sec $\pm$ 1% - uniform upstream flow velocity within a cross-sectional flow diameter of 5.0 cm - uniformity maintained within $\pm$ 1% of target velocity - flow acceleration/deceleration shall be controllable - direction of flow shall be perpendicular to the droplet support fiber
5.1.6	Operational Requirements	- allow at least 2 minutes after filling chamber to ensure gas temperature and pressure has stabilized - allow a 'droplet dwell time' of at least 10 sec to ensure all droplet motion imparted by droplet deployment and needle retraction has subsided - a 'near real time' downlink of the color camera video and the chamber gas pressure and temperature shall be provided - fuel vapor mole fraction of $<$ 0.005 in the atmosphere - mole fraction of product species from precious tests shall be $<$ 0.02(for each product species; e.g., CO, CO_2 , H_2O)
5.1.7	Microgravity Requirements	- acceleration levels less than $10^{-4} m/s^2$ on three axes - measurement accuracy shall be $10^{-6} m/s^2$ - frequency range shall be 0.01 $-$ 125 Hz - sampling rate shall be 2 $-$ 5 times the frequency

5.1.1 Test Fuels

FLEX-2 experiments use two different pure fuels and four different fuel mixtures. The pure fuels are a sooting alkane fuel (decane) and a nominally non-sooting alcohol fuel (ethanol). Investigations of sooting and non-sooting fuels allow us to quantify the influences of sooting on extinction and burning dynamics, such as radiative output. Also, the chemical kinetics of alkanes and alcohols are fundamentally different due to the presence of oxygen molecules in the alcohol which will help explain effects of fuels on the burning characteristics. In addition, since the Droplet Combustion Experiment 1 (DCE-1) and FLEX-1 experiments used a lower alkane (heptane) and a lower alcohol (methanol) these higher order alkane and alcohol test will help develop comprehensive chemical kinetic models for realistic fuels. These fuels have also been used in the FSDC and drop-tower experiments and extensive experimental data exist for smaller droplets. The fuel mixtures used in the experiments are heptane/hexadecane, propanol/glycerol, heptane/octane, and decane/propylbenzene. The mixtures are chosen to examine the liquid phase diffusion effects and to develop surrogate models for the aviation fuel JP8.

Fuel Type: Pure fuel droplets shall be decane ($C_{10}H_{22}$), an alkane fuel with a wide range of sooting behavior that varies depending on environmental conditions or ethanol (C_2OH), a non-sooting alcohol fuel. Mixed fuel droplets shall be either heptane/hexadecane, propanol/glycerol, heptane/octane, or decane/propylbenzene.

Fuel Purity: Purity levels shall be the highest purity level that is commercially available (research grade at 99.5% by volume at present) and all liquids shall be degassed and contain no H_2O.

Quality Assurance: Certification of test samples shall be provided prior to flight.

Fuel Temperature: Fuels shall be deployed at temperatures between 18 ^oC − 27 ^oC.

5.1.2 Droplet Deployment and Ignition

Droplet size during FLEX-2 experiments will vary between 1.5 mm and 5 mm. A measured quantity of fuel is dispensed from a fuel reservoir and deposited onto the support fiber using a suitable deployment technique (e.g., opposed-needle technique used in DCE or single-needle technique implemented in the ground-based rigs). Hot-wire igniters are positioned at the proper location for ignition prior to deployment. Following deployment, after a preset dwell time designed to allow droplet surface oscillations to die out, the gas-phase fuel/oxidizer mixture is ignited using minimum ignition energy. Our previous experimental results show that deployment-induced droplet surface oscillations die out within a second. The ignition system should be capable of waiting for a predetermined duration for the oscillations to die out. After ignition, a cylindrical zone of exclusion axially aligned with the flow and radially centered at the droplet deployment site and extending 20 droplet diameters downstream and at least 8 droplet diameters upstream in length from the droplet center and having a diameter of 10 initial droplet diameters must be maintained free of any objects.

Droplet size: Droplet diameters shall vary from 1.5 mm to 5 mm ± 0.25 mm.

Droplet reproducibility: Droplet size shall be reproducible to within ± 5%.

Support fiber: The support fiber diameter shall be less than 100 μm and shall serve to anchor the droplet at a fixed location.

Droplet Ignition: Ignition shall occur by hotwire ignition.

Igniter Positioning: The igniter tip shall be positioned within $0.5\,D_0 - 2.5\,D_0$ away from the anticipated droplet surface. The position of igniter tip shall be controllable by command to within $0.5\,mm$. The igniter tip shall be removed from viewing area upon ignition.

Igniter operation: The time of igniter power-up and duration of igniter operation shall be controllable by command and shall ignite the droplet with the *minimum ignition energy* necessary to sustain combustion.

Zone of exclusion: A spherical *zone of exclusion* of at least $10\,D_0$ extending radially in all directions from the droplet center must be maintained free of any objects (where D_0 is the initial droplet diameter). For non-quiescent tests (i.e., tests where a relative velocity between the ambient gas and the droplet is established) a cylindrical *zone of exclusion* shall be maintained that is axially aligned with the flow and radially centered at the deployment site extending volume of length $20\,D_0$ downstream, at least $8\,D_0$ upstream, and a diameter of $10\,D_0$ radially centered at the deployment site.

5.1.3 Initial Pressure

The ambient pressure changes the sooting and radiation characteristics of the droplet.

Ambient pressure: The initial ambient absolute pressure shall be set to $0.5\,atm - 3.0\,atm \pm 0.05\,atm$.

Pressure transient:: The chamber pressure shall be maintained within $\pm$ 10% the initial ambient pressure throughout each test.

5.1.4 Initial Ambient

The ambient oxygen mole fraction influences the burning rate, extinction diameter, flame chemistry and flame characteristics (size, temperature). This parameter will vary from 0.4 down to the limit where no flame can be sustained at any droplet diameter. The diluents used in the present study will be nitrogen and helium. Note that both nitrogen and helium are bio-compatible and helium help control the flame temperature.

Oxygen Mole Fraction: The oxygen mole fraction shall range from $0.1 - 0.4 \pm 0.005$.

Diluent Type: Diluents shall consist of either N_2 or He or a mixture of these two inert gases.

Diluent Mole Fraction: The diluent mole fractions shall vary depending upon the oxygen concentration specified for each test.

Ambient Quiescience: Gases shall be well-mixed and quiescent prior to ignition.

Ambient temperature: The initial chamber gas temperature shall be within $18\,^oC - 27\,^oC$.

Relative humidity: The chamber relative humidity shall be less than 10% for all the test points.

5.1.5 Ambient Flow Conditions

One objective of FLEX-2 is to study slow convective flow effects on burning characteristics. Procedures must be implemented to ensure flow uniformity. To establish the flow field the droplet-support fiber mechanism is translated at a specified speed. This method provides precise control over the imposed flow and allows accurate control of the flow acceleration/deceleration, particularly at low speeds.

During combustion the droplet continually shrinks in size and the Reynolds number, based on instantaneous droplet diameter, continually decreases if the flow velocity is not increased with time. In order to maintain a desired Reynolds number during combustion and to study flow induced transient effects we need to control the flow velocity with prescribed acceleration/deceleration values under certain test runs. Therefore the flow control system should have the capability to decelerate or accelerate.

Flow velocities: The target flow velocities shall be between 0.1 cm/sec to 5 cm/sec $\pm$ 1%.

Flow uniformity: The upstream flow field shall be uniform within a cross-sectional flow diameter of 5.0 cm and uniformity shall be maintained within $\pm$ 1% of target velocity.

Flow direction: The direction of the flow shall be perpendicular to the droplet support fiber.

Flow acceleration/deceleration: The flow acceleration/deceleration shall be controllable.

5.1.6 Operational Requirements

The chamber shall be filled with the appropriate atmosphere, which will vary in pressure between 0.5 atm to 3.0 atm and will vary in O_2 concentration between 0.1 to 0.4 mole fraction with the diluent gas making up the balance. A settling time of approximately 2 minutes will elapse prior to initiating the test in order to ensure that the temperature and pressure of the chamber gases have stabilized. This settling time will be followed by the dispensing of a predetermined amount of fuel (based on the target droplet size) onto the support fiber for those tests in which the droplet is not freely deployed. When sufficient fuel has been dispensed the dispensing needles will be retracted and a dwell period of at least 10 seconds will be allowed for the droplet internal fluid motion induced by deployment to subside. This will then be followed by initiating power to the igniter for a selectable amount of time ranging from 1 second to 5 seconds after which the igniter will be retracted from the field of view. If the flow field is to be generated by translating the droplet then droplet motion would commence at the same time that the igniter is retracted. A "near real-time" download of the color camera video will be required in order to verify successful droplet deployment, ignition, and overall progress of the experiment. Pressure and temperature data of the chamber environment will also be required in 'near real time'.

Gas stabilization time: After filling the chamber a stabilization period of at least 2 minutes shall be required to ensure that the chamber gas temperature and pressure have stabilized.

Droplet dwell time: Immediately following droplet deployment, a *dwell* time of up to 10 seconds shall be required to ensure all droplet motion imparted by droplet deployment and needle retraction has subsided. [1].

[1] This time may be insufficient for large droplets, at least for damping of internal flows. Also, internal flows within methanol droplets may never decay to low levels because of Marangoni effects (i.e., from water absorption)

Real time downlink: A 'near real time' downlink of the color camera video and the chamber's gas, pressure and temperature shall be provided.

Chamber atmosphere purity: The fuel vapor mole fraction shall be < 0.005 in the atmosphere prior to each test and the mole fraction of each product species (i.e., CO, CO_2 and other products) from any preceding tests shall be < 0.02.

5.1.7 Microgravity Requirements

In order to compare the experimental data with theoretical results obtained under the conditions when $Re \sim O(1)$ we need to minimize the effects of buoyancy on the flow field. The dimensionless parameter that compares the buoyancy effects to forced flow effects is the ratio of two dimensionless groups, the Gr/Re^2, where Gr is the Grashof number, and Re is the Reynolds number. The magnitude of this dimensionless group indicates the relative effect of buoyancy compared to forced convection. These experiments will require that $Gr/Re^2 << 1$ which translates into the following requirement for the g-level:

$$\frac{Gr}{Re^2} = \frac{g\,\beta\,\Delta T\,D}{U_\infty^2} << 1 \tag{2}$$

where g is the gravitational acceleration, β is the coefficient of thermal expansion, ΔT is the characteristic temperature difference, D is the characteristic length scale and U_∞ is the free-stream velocity. For the worst case scenario where $\beta \cdot \Delta T \sim 5$, $D \sim 1\,cm$ and $U_\infty \sim 1\,cm/s$ which suggests a g/g_0 value less than $1x10^{-5}$ as the required g-level (where g_0 is earth's normal gravity).

Micro-gravity levels: Accelerations are required to be less than $10^{-4} m/s^2$ within a frequency range of $0.01\,Hz - 125\,Hz$ in order to ensure buoyant forces are negligible. Measurements shall be made within an accuracy of $10^{-6} m/s^2$ at a sampling rate of $1-5$ times the frequency.

5.2 Diagnostic Requirements

This section describes the diagnostic requirements and the rationale behind the requirements. A table summarizing each of the diagnostic requirements is presented below and is followed by a detailed explanation of the rationale behind each of the requirements.

Table 6: Diagnostic requirements tabulation.

Section	Description	Requirements
5.2.1	Droplet Imaging	- focal plane parallel to support fiber - FOV at least 3.0 cm centered on droplet (center of FOV) - resolution of 30 μm for smallest droplet size over entire FOV - frame rate at least 30 fps - depth of view at least 3.0 cm - some tests may be run in $2x2$ binned mode (at $60 - 100$ fps) with a $\pm$ 60 μm spatial resolution - ability to backlight the droplet
5.2.2	OH^* Flame Imaging	- focal plane parallel to support fiber - FOV at least 5.0 cm centered on droplet (center of FOV) - color detection for wavelengths of 310 nm $\pm$ 5nm - resolution of 100 μm - frame rate at least 30fps - depth of view at least 3.0 cm - adjustable gain
5.2.3	Color Flame Imaging (Experiment Monitoring Camera)	- full flame view with focal plane parallel to support fiber (preferred) - FOV at least 5.0 cm and positioned such that entire flame is imaged - resolution of 100 μm - frame rate at least 30 fps - depth of view at least 3.0 cm - near real- time downlink

5.2.4	Flame Radiation	- radiometer used to detect water vapor radiation shall be filtered to detect wavelengths in a band centered at $1.87\,\mu m$ - radiometer used for broad-band radiation shall detect wavelengths within a band from $0.6 - 5.0\,\mu m$ - sample rate shall be at a frequency of $30\,Hz$ - radiometers shall be shielded from all reflected and/or direct radiation from the igniter wire - radiometers shall be positioned at least $15\,cm$ from the droplet to enable detection of all incident radiation from the flame - accuracy 5% of full scale incident radiation - response time constant to be $<\ 40\,ms$ - field of view shall be $65\,mm$ diameter centered around the deployment site
5.2.5	Soot Volume Fraction	- camera shall provide full view of the droplet and flame with a preferred orientation such that the focal plane is parallel to the flow direction and coplanar with the droplet - backlit with wavelength of $660\,nm$ and a FWHM of $5\,nm$ - frame rate of $15\,fps$ - FOV at least $5\,cm$ about center of deployed droplet - resolution of $50\,\mu m$ over the entire FOV
5.2.6	Soot/Fiber Temperature	- focal plane shall be parallel to the flow direction and coplanar with and centered on the droplet - FOV at least $5\,cm$ about the center of the deployed droplet - at least $7\,fps$ for both wavelengths - resolution of $50\,\mu m$ over the entire FOV - shall be adjustable prior to each test
5.2.7	Flow Velocity Measurement	- record translated motion (accelerated and steady) - sample rate shall be $\geq\ 30\,Hz$

5.2.8	Ambient Pressure and Temperature Measurement	- minimum sample rate shall be at 10 Hz - temperature accuracy shall be at least $\pm 0.5\,C$ in the range of $18 - 27\,C$ - pressure accuracy shall be at least $\pm 0.01\,atm$ in the range of $0.5 - 3.0\,atm$
5.2.9	Time Synchronization	- all measurements shall be referenced to GMT with a minimum accuracy of $\pm 0.03\,sec$

5.2.1 Droplet Imaging

A back-lit view of the droplet shall be provided that will allow accurate measurements of the droplet size as a function of time. This is necessary to obtain droplet burning rates and extinction droplet diameters. This view also yields quantitative information regarding the soot shell and soot shell dynamics. The time resolution is necessary to accurately measure the burning rate constant and it's temporal variation as well as accurate measurements of the extinction droplet diameter.

Orientation: The focal plane shall be aligned so that it is parallel with the fiber support axis and coplanar with the droplet.

Field of view: The FOV shall not exceed 3.0 cm centered about the droplet.

Spatial resolution: The spatial resolution shall be $30\,\mu m$ (i.e. $> 16\,lp/mm$) for the smallest droplet size over the entire FOV. If higher than nominal framing rates are requested for specific tests (i.e.,from 60-100 fps) then the spatial resolution shall be $60\,\mu m$(i.e. $> 8\,lp/mm$).

Minimum frame rate: The nominal minimum frame rate shall be 30 fps over the duration of the test unless a faster frame rate (i.e., between $60\,fps - 100\,fps$) is requested.

Depth of view: The depth of view shall be no less than $3.0\,cm$.

Illumination: The droplet shall be 'backlit' with a uniform collimated light source of sufficient intensity to allow the droplet's edge to be clearly detected.

5.2.2 $OH*$ Flame Imaging

The flame structure and its dynamic response shall be obtained from the flame imaging camera oriented perpendicular to the stream-wise flow direction (i.e,. the flow direction shall be parallel with the image plane). The flame image shall be derived from the ultraviolet OH-radical chemiluminescence emission intensity. This technique is well understood and has been implemented in a previous flight experiment (DCE-1).

Orientation: The focal plane shall be parallel to the flow direction.

Field of view: The flame FOV shall be no less than $5.0\,cm$.

Depth of view: The depth of view shall be no less than $3.0\,cm$.

Color: The flame imaging camera shall be capable of detecting wavelengths of $310nm \pm 5nm$ using an intensified camera in order to detect $OH*$ radical emission.

Spatial resolution: The spatial resolution of the flame imaging camera shall be 100 μm (i.e. $>$ 5 lp/mm) over the entire FOV.

Minimum frame rate: The frame rate shall be 30 fps over the duration of test.

Gain setting: The gain shall be adjustable prior to each test.

5.2.3 Secondary Color Flame Imaging

A color CCD camera viewing the droplet at a specified angle will provide flame color information during combustion. Based on earlier flight experiments, it is also desired that this camera serve as the experiment's monitor camera to facilitate experiment operation/monitoring from the ground.

Orientation: The color camera shall provide full view of the droplet and flame with the focal plane parallel to the flow direction preferred; this camera shall provide viewing of the droplet dispensing and deployment sequence.

Field of view: The FOV shall be at least 5.0 cm.

Depth of view: The depth of view shall be at least 3.0 cm.

Minimum frame rate: The frame rate shall be 30 fps over the duration of the test.

Downlink: The images shall be down-linked to the PI in *near real-time* during each test.

Zoom: A 'zoom' capability shall be provided, upon request by the PI (allowing for a commensurate decrease in FOV) in the event that a more detailed view of the deployment, ignition and burning process is required.

5.2.4 Flame Radiation

Prior experimental results from DCE and FSDC have established that both luminous and non-luminous radiation play a significant role in flame extinction. These measurements will be used to obtain the total radiant energy loss as well as to establish the exact moment of flame extinction and to supplement other imaging data in determining transient flame behavior. Thermopile radiometers, positioned at distances far enough from the droplet to allow full view of the flame, will be used to measure *broad-band* radiation and water-vapor radiation from the flame zone.

Water vapor: The radiometer used to detect water vapor radiation shall be filtered to detect wavelengths in a band centered at 1.87 μm (5.1 μm $-$ 7.5 μm)

Broad-band spectrum: The radiometer used for broad-band radiation shall detect wavelengths within a band from 0.6 μm $-$ 5 μm.

Sample rate: Data sampled from the radiometer shall be at a frequency of 30 Hz.

Positioning: The radiometers shall be positioned at least 15 cm from the droplet to enable detection of all incident radiation from the flame.

Field of view: The FOV of at least 65 mm shall be centered on the droplet deployment site.

Response Time: The radiometers shall have a time constant of less than 40 ms.

Accuracy: The radiometers shall be accurate to within 5% of the estimated full scale incident radiation.

5.2.5 Soot Volume Fraction Measurement

It has long been established that the presence of soot will influence the droplet burning rate, the flame dynamics, and the flame extinction limits. Increased thermal radiation from the soot forming region, impacts on mass and thermal diffusion due to the physical presence of soot acting as a barrier to the diffusive processes, and the changes in thermophysical properties in the fuel-rich region of the diffusion flame due to varying levels of soot concentration all contribute to changes in the dynamics of the droplet burning and extinction behavior. In order to assess these influences with the n-heptane droplet tests it is *desired* to quantify soot concentration levels by obtaining soot volume fraction measurements within the diffusion flame.

An established technique for making this measurement has been to use a multi-chord, line-of-sight light extinction measurement coupled with an inversion technique to obtain soot volume fraction distributions. This requires a backlight using a collimated laser light source of known intensity and by discriminating that intensity from the flame emission and stray light by using combinations of interference and neutral density filters. It is anticipated that this measurement, if available, will use the HiBMS camera with the appropriate spectral filtering, typically 660 nm with a FWHM (full width half maximum) of 5 nm, and with an appropriate intensity resolution, which typically requires a minimum of 8 bits of dynamic range.

Orientation: The camera used for SVF measurements shall provide a full view of the droplet and flame with a preferred orientation such that the focal plane is parallel to the flow direction and coplanar with the droplet center.

Backlit illumination: A collimated light source with a wavelength of 660 nm and a FWHM of 5 nm shall be provided.

Frame rate: The frame rate shall be at least 15 fps.

Field of view: The FOV shall be at least 5.0 cm x 5.0 cm.

Resolution: The resolution shall be 50 μm (i.e. $>$ 10 lp/mm) over the entire FOV.

5.2.6 Soot/Fiber Temperature

In addition to knowing the soot volume fraction it is equally important to know the soot temperature. Therefore, it is *desired* to quantify the soot temperature (and SiC fiber temperature) to obtain quantitative information regarding the broadband radiation due to soot.

An established technique for making soot temperature measurements, which has been successfully implemented in ground-based facilities, is by use of multi-wavelength pyrometry. This measurement will use the CIR HiBMS camera with the Liquid Crystal Tunable Filter (LCTF) since limitations of the CIR/MDCA hardware will preclude two cameras simultaneously imaging different wavelengths. The framing rate of the single HiBMS camera, combined with a rapid temporal response of the LCTF, will make it feasible to make measurements on successive frames at two different wavelengths. Assuming minimal changes in soot volume fraction and temperature during the inter-frame time, it will be possible to measure soot temperature. Additionally, this

system will be used to measure the temperature of the SiC support fiber (during non-sooting tests) as a proxy for the gas-phase flame temperature.

Orientation: The camera shall provide full view of the droplet and the flame with a preferred orientation such that the focal plane of the camera is parallel to the support fiber.

Frame Rate: The frame rate shall be at least 7 fps.

Field of View: The FOV shall be at least 5.0 cm x 5.0 cm about the center of the deployed droplet.

Resolution: The resolution shall be 50 μm (i.e. $>$ 10 lp/mm) over the entire FOV.

5.2.7 Flow Velocity Measurement

It is important that the instantaneous relative free-stream velocity is known accurately during the entire combustion process. If measurements are not feasible an indirect feed-back related to velocity through calibration should be provided. If the relative velocity is established by translating the droplet then information providing position with time will be required. In either case a sampling frequency of at least 30 Hz shall be required.

Sample Rate: Velocity and/or droplet position data shall be provided at a frequency of at least 30 Hz.

5.2.8 Ambient Temperature and Pressure Measurement

During each test the chamber gas temperature and pressure measurements shall be required. The following are the specifications for this data.

Sample rate: The frequency of chamber temperature and pressure data shall be 10 Hz.

Temperature: Temperatures shall be accurate to within $\pm\, 0.5^o\, C$.

Pressure: Pressures shall be accurate to within $\pm\, 0.01\, atm$ in the range of $0.5 - 3.0\, atm$.

5.2.9 Synchronization

Experiment objectives require all data to be time-synchronized to a reference time. This will allow accurate interpretation of the data and will allow evaluation of droplet regression rate, flame structure, and flame extinction as a function of time.

Time synchronization: All measurements shall be referenced to GMT and shall be accurate to within $\pm\, 0.03\, sec$.

5.3 Flight Experiment Test Procedures

The FLEX-2 experiments involve igniting and observing the burning behavior of relatively large droplets in a preselected ambient condition. The primary objectives of the experiments are to study the fundamental burning characteristics of sooting and non-sooting pure fuels and fuel mixtures. The effects of slow convection and the droplet-droplet interactions associated with droplet pairs are also examined. The basic procedures of a typical experimental run will be as follows:

1. Select the test pressure, oxygen/diluent mixture concentration and fill the combustion chamber.
2. Allow, at a minimum, approximately two minutes for the ambient gas to reach quiescence.
3. Energize the diagnostic devices and start the recording process and ensure that there is a live down-link of the color camera
4. Select the droplet's initial size and deploy the droplet (or droplets) in either a free-floated or tethered mode.
5. Wait few seconds for droplet deployment induced velocities to die down.
6. Ignite and observe the combustion process.
7. If the chamber environment, following a combustion event, permits a subsequent run then repeat steps 3 through 6; if not, then start from step 1.

5.4 FLEX-2 Test Matrix

A detailed test matrix, pursuant to on-going ground testing, will be developed during the coming years to meet the stated science objectives and at the same time meet the constraints imposed by the flight hardware and the safety requirements of space station operations. The exact test matrix will potentially change during the conduct of the FLEX-2 experiment. The extensive ground testing in the drop towers at the NASA Glenn Research Center and the results from the FLEX experiments will provide information to help finalize the final test matrix. It is important, however, for the engineering team to have a preliminary test matrix envelope in order to estimate consumables and prepare for the necessary safety reviews. This test matrix envelop is presented in Section 4.3 for this purpose.

6 Post-Flight Data Analysis

The data obtained from the flight experiments are in the form of video images and text data sampled and stored at a specific time intervals. The video images consist of back-lit droplet view, OH* emission views, and color camera views, all obtained at 30 fps. However, when needed the droplet view camera will be operated up to 100 fps. The radiometer data is stored in text form and sampled at 100 Hz. The combustion chamber temperature and pressure are also measured and stored during each experimental run and they are available for data interpretation if needed. Form these raw data a number of quantitative flame characteristics are extracted using image analysis and other mathematical analysis tools.

Specific analyses and model(s)-to-experiment comparisons to be performed include, but are not limited to the following list:

- Droplet diameter as a function time and burning rate constant
- Flame diameter as a function of time
- Droplet diameter at flame extinction
- Flame diameter at extinction
- Soot volume fraction as a function of time
- Soot-shell dynamics
- Radiant emission from the flame
- Effects slow convection on the items mentioned above
- Effects of tethering on the items mentioned above

6.1 Science Success Criteria

In order to gauge the level of experimental success, criteria for two levels of success - minimal and complete success - have been defined in this section. Minimal Success requires that the measurements listed below are successfully obtained for a sufficiently representative set of test points to the extent that some meaningful conclusions related to the Science Objectives, as defined in Section 4, can be made. Complete Success requires that all the measurements listed below, for a sufficiently representative set of test points, are successfully obtained.

6.1.1 Minimal Success

In order for the flight experiment to be considered minimally successful, the FLEX-2 team must acquire a minimal set of data to allow validation of the theoretical/numerical models over a minimal range of ambient conditions. There must be sufficient data to allow for at least two of the four categories of experiments, namely, pure fuel experiments, fuel mixture experiments, convective effects experiments, and droplet arrays experiments, have the following measurements:

- Obtain droplet diameter and either $OH*$ or color video flame measurements as function of time at two pressures over a range of droplet sizes and oxygen concentrations.

This criteria essentially states that sufficient data is collected for two of the four categories of experiments to make meaningful scientific conclusions in the form of a technical publication.

6.1.2 Complete Success

In order for the complete success criteria to be met the following measurements, are required for three of the four categories of experiments:

- Droplet diameter and flame diameter as function of time for a range of initial diameter, oxygen concentration, and pressure.
- Radiometer data for the same range of conditions.
- For convective effects experiments at least five different initial Reynolds number conditions.
- For arrays experiments two different L/D ratios or two different diluent conditions for the same L/D ratio.

6.2 Hardware Success Criteria

Hardware success is also defined at a minimal and complete level and is determined by the required functionality of the hardware to meet the same Science Success Criteria defined above. Discussion of the hardware is limited to those components and/or systems that are specific to this experiment's diagnostics and/or operation and as such does not include discussion of hardware operability that may be considered more global in application (e.g., FOMA, data storage and retrieval systems, etc.).

6.2.1 Minimal Success Criteria

The following components need to function successfully in order to meet the minimal success criteria.

- CIR Laser Illuminating Package used for droplet backlighting and the CIR HFR/HR used for imaging the droplet imaging.
- MDCA color camera used for flame imaging in the visible spectrum.
- All components required for successfully dispensing, deploying on a fiber, and igniting the droplets.
- All components required for establishing and measuring the full range of flow velocities.
- All components required to deploy a binary linear droplet array.

6.2.2 Complete Success Criteria

In addition to the required hardware functionality listed above for minimal success the following provides a list of the functionality required for complete success:

- Free deployment of droplets with initial sizes greater than 2 mm.
- UV imaging camera views at 30 fps.
- Radiometer data at 100 Hz for both broad band and narrow band.

7 Ground-Based Research Program

The ground based experimental and theoretical studies form a subset of the overall FLEX-2 flight experimental program. The ground-based studies help in interpreting the flight results over an wider range of time and length scales pertinent to droplet combustion. The following subsections outline the planned experimental and analytical research in support of FLEX-2. There are four primary objectives to the ground-based FLEX research program. The first goal is to use the drop towers and reduced gravity aircraft (when appropriate) to develop the procedures and hardware settings necessary to ensure satisfactory operation on orbit. This portion of the ground-based program is typically handled by the engineering team and is not covered by this document. The second component is to take data that will be used to determine the final FLEX-2 test matrix. The third component of the ground-based research program is to perform experiments to compliment the flight-based data (typically with smaller initial droplet sizes). The final component of the ground-based research program is the development of the theoretical and numerical tools necessary to extend and generalize the results of droplet combustion experiments to a wider range of fuels and environments.

7.1 Experiments

Currently three drop-tower capable (2.2 second tower and the 5 second zero gravity facility) microgravity droplet combustion experimental rigs are available to support the FLEX-2 experimental program, namely, Bi-component rig (UC, Davis), Sooting droplet rig (Drexel), and Convective droplet rig (NASA/NCSER). These rigs are capable of freely deploying the droplet and igniting them at various pressures and ambient environments. Tethered droplets with an imposed slow convective velocities can also be studied using one of the rigs. Modification will be made to the droplet translating, fiber-supported droplet combustion rig to study droplet array combustion. An additional experimental rig suitable for the one second drop facility at Cornell will be modified and fitted with digital imaging systems for experiments at Cornell focussed on surrogate fuel studies.

7.2 Theoretical and Numerical Studies

Theoretical and numerical models help to generalize the experimental observation to a wider range of conditions encountered in practical applications. As described in Section 3, each team member has specific scientific objectives and is responsible for the theoretical and/or numerical model development. Some of the planned activity in this area are described below. FLEX-2 research program will examine diffusive transport in detail with the goal of validating and improving diffusive transport models for use in theoretical and numerical simulations of droplet combustion with multicomponent liquid fuels. Particular emphases will be to examine the influences of Soret transport and multicomponent diffusion effects on transport of species to and from flame zones, e.g., through appropriate modeling of Lewis numbers, with the resulting influences on transient combustion behaviors (e.g., burning rates and flame standoff ratios), radiant heat transfer, extinction, LOI conditions and sooting. The modeling approaches will be analytical, using asymptotic methods, as well as computational, where detailed models for transport will be included in existing codes. Where appropriate, reduced chemical kinetic models for the various fuels will be developed and expanded as done in the previous flight experiment programs (DCE and FLEX). Numerical models with detailed chemistry along with experimental data will be used to validate the reduced chemical kinetic schemes. Theoretical models for other aspects of droplet combustion such as the effects of slow convection and droplet-droplet interactions will also be developed during this study.

8 Science Management Plan

The FLEX-2 Research Team Lead, F.A. Williams, maintains overall responsibility for the FLEX-2 research program. All major decisions regarding the FLEX-2 flight experiment and ground-based research program rest with the Research Team Lead. It is fully expected, however, that all of the external and internal GRC investigators will have a great deal of autonomy in the *day to day* operations of their own research. This includes the preparation of test plans and conducting experiments and analyzing and reporting the resulting data. All of the participating will meet and talk periodically to discuss flight hardware developments, research results and discuss relevant issues. All team members will report the results of their results to NASA in the form of periodic progress reports and more importantly to the peer community in technical meetings and journal publications. The Research Team Lead is responsible for the reporting the results of the overall research at the conclusion of the FLEX-2 project. Table shows the primary responsibility of each of the team members.

Table 7: Specific Roles and Areas Responsibility of FLEX-2 Researchers.

Investigator	Role	Area of Research
F. A. Williams	PI and Team Lead	Theoretical Model Development
NASA Research Team		
D. Dietrich and P. Struk	Co-Is	Droplet Arrays Combustion
M. Hicks and V. Nayagam	Co-Is	Radiation and Slow Convection Effects
External Research Team		
C. T. Avedisian	Co-I	Real Fuel Experiments
M. Y. Choi	Co-I	Soot Formation
F. L. Dryer	Co-I	Numerical Model Development
B. D. Shaw	Co-I	Liquid Phase Phenomena

The primary *day to day* responsibility for the flight hardware rests with the GRC investigators, V. Nayagam and M. Hicks. The are responsible for the daily interactions with the hardware development team, reviewing flight hardware performance documentation and test results and supervising the ground-based experiments that impact the development of the detailed test matrix and flight hardware. The internal investigators will keep the entire FLEX-2 team updated on the results of testing and status of the flight hardware. Any critical decisions regarding the flight experiments are the responsibility of the Research Team Lead in consultation with all of the FLEX-2 team members.

The analysis of the ground-based data will be the responsibility of the researcher who acquires the data. The analysis of the flight data will be jointly performed by the entire FLEX-2 team under the direction of the FLEX-2 Research Team Lead. The archiving of the flight experimental data in an open-source, publicly available format will be the responsibility of the GRC team members under the supervision of the FLEX-2 Research Team Lead.

The development of the detailed numerical model will be the responsibility of F.L. Dryer. This includes code development, incorporation of *state of the art* sub-models of radiation, chemical kinetics, transport, etc. and validation of the model against both the space-flight and ground-based data.

9 Justification for Reduced Gravity

The objective of this experiment is to use the droplet as a model geometry for investigating suppressant agent efficacy. In order to completely leverage the droplet geometry, it is critically important to maintain spherical symmetry throughout the test. This can only occur if the diffusive residence times (i.e., mass (τ_m) and thermal (τ_k) are much lower than the buoyancy-controlled residence time (τ_b). Using the droplet diameter (D) as the characteristic length the expressions for the ratio of these two characteristic times to the buoyancy controlled residence time are

$$\frac{\tau_k}{\tau_b} = \frac{\sqrt{g\,D^3}}{\alpha_g} \tag{3}$$

and

$$\frac{\tau_m}{\tau_b} = \frac{\sqrt{g\,D^3}}{\mathcal{D}_g} \tag{4}$$

where α_g and $\mathcal{D}_g$ are the thermal and mass diffusivities of the gas phase. In order to justify neglecting buoyant effects the above ratios must be much lower than unity. This is only accomplished by changing at least one of the three independent variables, droplet diameter, pressure or gravity level (or some combination of the three).

Experiments in 1-g environments, performed in pressures of 1 atmosphere, require droplet diameters substantially smaller than 1 mm. This makes key diagnostics impractical since the image resolution begins to approach the dimensions of the distances being measured (e.g., flame standoffs, droplet regression, thin filament pyrometry). Also, the present experiment requires finite and measurable extinction droplet diameters (and a period of near quasi-steady burning prior to extinction) in order to quantify the influence of finite rate chemistry. The droplet diameters required to minimize buoyancy effects are small enough that extinction droplet diameters would either not be practically measurable or, more likely, not even exist.

Since diffusivities are inversely proportional to pressure the residence time ratios could alternatively be reduced by reducing test pressures. Chung and Law (1986) used this approach to measure extinction droplet diameters and from that determine single step chemical kinetic constants for decane in normal gravity. The range of oxygen concentrations and pressures was, however, very limited. Studying such a small range of droplet diameters, pressures and oxygen concentrations would severely limit the ability to achieve the stated objectives of the present study. Furthermore, Easton (1998) showed that the conditions that yielded finite extinction diameters in the work of Chung and Law (1986) burned to completion (no flame extinction) in microgravity. The author attributed this to a small residual buoyant-flow that is large enough in the vicinity of the flame to influence the extinction process (Struk et al., 1997).

The need for extended duration microgravity facilities is predicated on the fact that the burn-to-completion time for large droplets is longer than the time available in the ground-based facilities. Typically the droplet life-time (τ_l) can be estimated from the initial droplet size (D_0) and the average burning rate constant (k) as $\tau_l = \frac{D_0^2}{k}$. The values of τ_l for n-heptane, and methanol droplets burning in air at one atmospheric pressure range from 10 to 30 s for initial droplet diameters in the range 3 to 5 mm assuming an average burning rate constant of 0.8 mm^2/s. Moreover, high fidelity experiments demand additional microgravity time for droplet deployment, droplet quiescence, and ignition. Experiments involving radiative extinction require that the droplets be ignited in microgravity. Such experimental requirements also lead us to employ larger droplets, which in turn necessitates long-duration microgravity facilities. Both Dietrich et al. (2005) and

Easton (1998) studied extinction of single droplets in drop towers. Dietrich et al. (2005) used the Japan Microgravity Center 10 *s* drop tower, a facility no longer available, and even then could only study a limited parameter space because of the limited microgravity time. Therefore, the only facility which will enable data of sufficient quality over a wide parameter space is the microgravity environment available in extended-duration microgravity facilities (i.e. Space Shuttle or ISS).

References

Ackerman, M., Colantonio, R. O., Crouch, R. K., Dryer, F. L., Haggard, J. B., Linteris, G. T., Marchese, A. J., Nayagam, V., Voss, J. E., and Williams, F. (2003). A treatment of measurements of heptane droplet combustion aboard MSL-1. NASA-TM 2003-212553.

Ackerman, M. D. and WIlliams, F. A. (2005). A simplified model for droplet combustion in a slow convective flow. *Combustion and Flame*.

Aharon, I. and Shaw, B. D. (1996). Marangoni instability of bi-component droplet gasification. *Physic of Fluids*, 8:1820–1827.

Aharon, I. and Shaw, B. D. (1998). Estimates of liquid species diffusivities from experiments on reduced-gravity combustion of heptane-hexadecane droplets. *Combustion and Flame*, 113:507–518.

Annamalai, K. (1995). Interactive processes in evaporation and combustion of liquid drop arrays and clouds. In Chiu, H. H. and Chigier, N., editors, *Mechanics and Combustion of Droplets and Sprays*, pages 116–160. Begell House, Inc.

Annamalai, K. and Ryan, W. (1992). Interactive processes in gasification and combustion. part i: Liquid drop arrays and clouds. *Progress in Energy and Combustion Science*, 18:221–295.

Avedisian, C. T. (2000). Recent advances in soot formation from spherical droplet flames at atmospheric pressure. *Journal of Power and Propulsion*, 16(4):628–635.

Bae, J. and Avedisian, C. (2004). Experimental study of the combustion dynamics of jet fuel droplets with additives in the absence of convection. *Combustion and Flame*, 137(1-2):148 – 162.

Bae, J. H. and Avedisian, C. T. (2005). Soot emissions from spherical droplet flames for mixtures of jp8 and tripropylene glycol monomethyl ether. *Environmental Science and Technology*, 39(20):8008 – 8013. Soot dynamics;Droplet flames;Soot emissions;Droplet diameters;.

Bressloff, N., Moss, J., and Rubini, P. (1996). Cfd prediction of coupled radiation heat transfer and soot production in turbulent flames. *Proceedings of the Combustion Institute*, 26:2379 – 2386. Droplet combustion ; Soot.

Chen, A. and Shaw, B. (2000). Laser attenuation measurements of soot volume fractions during reduced-gravity combustion of heptane and heptane/hexadecane droplets. *Combustion Science and Technology*, 150(1):59 – 75. Reduced gravity combustion;Hexadecane;Soot volume fractions;.

Chiu, H. H. (2000). Advances and challenges in droplet and spray combustion: Toward a unified theory of droplet aerothermochemistry. *Progress in Energy and Combustion Sciences*, 26:381–416.

Choi, M. Y. and Dryer, F. L. (2001). Microgravity droplet combustion. In Ross, H. D., editor, *Microgravity Combustion: Fire in Free Fall*, Combustion Treatise, chapter 4, pages 183–297. Academic Press.

Choi, M. Y., Dryer, F. L., and Haggard, J. B. (1990a). Observations on a slow burning regime for hydrocarbon droplets: n-heptane/air results. *Proceedings of the Combustion Institute*, 23:1597–1604.

Choi, M. Y., Dryer, F. L., and Jr., J. B. H. (1990b). Observations on a slow burning regime for hydrocarbon droplets: n-heptane/air results. *Proceedings of the Combustion Institute*, 23:1597–1605.

Choi, M. Y. and Lee, K.-O. (1996). Investigation of sooting in microgravity droplet combustion. *Proceedings of the Combustion Institute*, 26:1243 – 1249.

Chung, S. H. and Law, C. K. (1986). An experimental study of droplet extinction in the absence of external convection. *Combustion and Flame*, 64:237–241.

Colket, M., Edwards, T., Williams, S., Cernansky, N. P., Miller, D. L., Egolfopoulos, F., Lindstedt, P., Seshadri, K., Dryer, F. L., Law, C. K., Friend, D., Lenhert, D. B., Pitsch, H., Sarofim, A., Smooke, M., and Tsang, W. (Jan 8-11, 2007). Development of an experimental database and kinetic models for surrogate jet fuels. In *AIAA Paper 2007-0770*, Reno, NV, United States.

Cooke, J. A., Bellucci, M., Smooke, M. D., Gomez, A., Violi, A., Faravelli, T., Ranzi, E., and Quintiere, J. (2005). Computational and experimental study of jp-8, a surrogate, and its components in counterflow diffusion flames. *Proceedings of the Combustion Institute*, 30:439 – 446.

Crespo, A. and Liñan, A. (1975). Unsteady effects in droplet evaporation and combustion. *Combustion Science and Technoaly*, 11:9–18.

Dietrich, D. L., Haggard, J. B., Dryer, F. L., Nayagam, V., Shaw, B. D., and Williams, F. A. (1996). Droplet combustion experiments in spacelab. *Proceedings of the Combustion Institute*, 26:1201–1207.

Dietrich, D. L., Struk, P. M., Ikegami, M., and Xu, G. (2005). Single droplet combustion of decane in microgravity: Experiments and numerical modeling. *Combustion Theory and Modeling*, 9(4):569–585.

Dwyer, H. and Sanders, B. R. (1986). A detailed study of burning of fuel droplets. *Proceding of the Combustion Institute*, 21.

Dwyer, H. and Sanders, B. R. (1988). Calculations of unsteady reacting droplet. *Proceding of the Combustion Institute*, 22:1923–1929.

Dwyer, H. A., Aharon, I., Shaw, B. D., and Niazmand, H. (1996). Surface tension influences on methanol droplet evaporation in the presence of water. *Proceedings of the Combustion Institute*, 26:1613–1619.

Dwyer, H. A., Shaw, B. D., and Niazmand, H. (1998). Droplet/flame interactions including surface tension influences. *Proceedings of the Combustion Institute*, 27:12–16.

Easton, J. W. (1998). Large diameter, radiative extinction experiments with decane droplets in microgravity. Master's thesis, Case Western Reserve University, Cleveland, Ohio 44106.

Edwards, T. and Maurice, L. Q. (2001). Surrogate mixtures to represent complex aviation and rocket fuels. *Journal of Propulsion and Power*, 17(2):461–466.

Eisenklam, P., Arunachalam, S., and Weston, J. (1967). Evaporaion rates and drag resistance of burning drops. *Proceedings of the Combustion Institute*, 11:715–728.

Faeth, G. (1977). Current status of droplet and liquid combustion. *Progress in Energy and Combustion Sciences*, 3:191–224.

Fendell, F., Sprankle, M., and Dodson, D. (1966). This-flame theory for a fuel droplet in slow viscous flow. *Journal of Fluid Mechanics*, 26(2):267–280.

Frenklach, M. and Wang, H. (1991). *Proceedings of the Combustion Institute*, 23:1559–1566.

Frenklach, M. and Wang, H. (1994). *Detailed mechanism and modeling of soot particle formation*, pages 165 – 192. Number 59. Polycyclic aromatic hydrocarbons;Surface growth;Mathematical formalism;Chemical processes;Physical processes;.

Frossling, N. (1938). Evaporation of falling drops. *Gerlands Beitr. Geophys.*, 52:170–216.

Godsave, G. A. E. (1952). Studies of the combustion of drops in a fuel spray - the burning of single drops of fuel. *Proceedings of the Combustion Institute*, 4:818–830.

Gogos, G. and Ayyaswamy, P. S. (1988). Model for the evaporation of a slowly moving droplet. *Combustion and Flame*, 74(2):111 – 129.

Gogos, G., Sadhal, S. S., Ayyasamy, P. S., and Sundararajan, T. (1986). Thin-flame theory for the combustion of a moving liquid drop: Effects due to variable density. *Journal of Fluid Mechanics*, 171:121–144.

Gokalp, I., Chauveau, C., Richard, J. R., Kramer, M., and Lueckel, W. (1988). Observation on the low temperature vaporization and envelope or wake flame burning of n-heptane droplets at reduced gravity during parabolics flights. *Proceedingss of the Combustion Institute*, 22:2027–2035.

Goldsmith, M. (1956). Experiments on the burning of single drops of fuel. *Jet Propulsion*, 26:628–635.

Hakansson, A., Stromberg, K., Pedersen, J., and Olsson, J. (2001). Combustion of gasolines in premixed laminar flames european certified and california phase 2 reformulated gasoline. *Chemosphere*, 44(5):1243 – 1252.

Hall, A. R. and Diederichsen, J. (1953). An experimental study of the burning of single drops of fuel in air at pressures up to twenty atmospheres. *Proceedings of the Combustion Institute*, 4:837–846.

Hanson, S. P., Beer, J. M., and Sarofim, A. F. (1982). Non-equilibrium effects in the vaporization of multicomponent fuel droplets. *Proceedings of the Combustion Institute*, 19:1029–1036.

Huang, L. W. and Chen, C. H. (1998). Numerical analysis of burning droplet with internal circulation in a gravitational environment. *Numerical Heat Transfer, Part A*, 34:43–60.

Isoda, H. and Kumagai, S. (1958). New aspects of droplet combustion. *Proceedings of the Combustion Institute*, 7:523–531.

Jackson, G. and Avedisian, C. (1994). The effect of initial diamter in spherically symmetric droplet combustion of sooting fuel. *Proceedings of the Royal Society of London A*, 446:255–276.

Jackson, G., Avedisian, C., and Yang, J. (1991). Soot formation during combustion of unsupported methanol/toluene mixture droplets in microgravity. *Proceedings of The Royal Society of London, Series A: Mathematical and Physical Sciences*, 435:359 – 369.

Jackson, G. S., Avesisian, C. T., and Yang, J. C. (1992). Observations of soot during droplet combustion at low gravity: heptane and heptane/monochloroalkane mixtures. *International Journal of Heat and Mass Transfer*, 35(8):2017–2033.

Jog, M. A., Ayyaswamy, P. S., and Cohen, I. M. (1996). Thin-flame theory for the combustion of a moving liquid drop: effects due to variable density. *Journal of Fluid Mechanics*, 307:135–165.

Kumagai, S. (1956). Combustion of fuel droplets in falling chambers with special refernce to the effect of natural convection. *Jet Propulsion*, 26:786.

Kumagai, S. and Isoda, H. (1956). Combustion of fuel droplets in a falling chamber. *Proceedings of the Combustion Institute*, 6:726–731.

Kumar, S., Ray, A., and Kale, S. (2002). A soot model for transient, spherically symmetric n-heptane droplet combustion. *Combustion Science and Technology*, 174(9):67 – 102.

Law, C. (1982). Recent advances in droplet vaporization and combustion. *Progress in Energy and Combustion Sciences*, 8(3):171–201.

Law, C. and Williams, F. (1972). Kinetics and convection in the combustion of alkane droplets. *Combustion and Flame*, 19(3):393–405.

Lee, K., Manzello, S., and Choi, M. (1998). The effect of initial diamter on sooting and burning behavior of isolated droplets under microgravity conditions. *Combustion Science and Technology*, 132:139–156.

Leung, K., Lindstedt, R., and Jones, W. (1991). A simplified reaction mechanism for soot formation in non-premixed flame. *Combustion and Flame*, 87:289 – 305. Droplet combustion ; Soot.

Manzello, S. L., Choi, M. Y., Kazakhov, A., Dryer, F. L., Dobashi, R., and Hirano, T. (2000). Sooting behavior of large droplets in the jamic facility. *Proceedings of the Combustion Institute*, 28:1079–1086.

Megaridis, C. M. (1993). Liquid-phase variable property effects in multicomponent droplet evaporation. *Combustion Science and Technology*, 92:291–311.

Mikami, M., Kato, H., Sato, J., and Kono, M. (1994). *Proceedings of the Combustion Institute*, 25:431.

Miyasaka, K. and Law, C. K. (1981). Combustion of strongly-interacting linear droplet arrays. *Proceedings of the Combustion Institute*, 18:283–292.

Moss, J. B., Stewart, C. D., and Sayed, K. J. (1988). Flowfield modelling of soot formation at elevated pressure. *Proceedings of the Combustion Institute*, 22:413 – 423.

Nayagam, V., Haggard, J. B., Colantonio, R. O., Marchese, A. J., Dryer, F. L., Zhang, B. L., and Williams, F. A. (1998). Microgravity n-heptane droplet combustion in oxygen-helium mixtures at atmospheric pressure. *AIAA Journal*, 36(8):1369–1378.

Niazmand, H., Shaw, B. D., Dwyer, H. A., and Aharon, I. (1995). Effects of marangoni convection on transient droplet evaporation. *Combustion Science and Technology*, 103:219–233.

Okajima, S. and Kumagai, S. (1974a). Further investigations of combustion of free droplets in a freely falling chamber including moving droplets. *Proceedings of the Combustion Institute*, 15:401–407.

Okajima, S. and Kumagai, S. (1974b). Further investigations of combustion of free droplets in a freely falling chamber including moving droplets. *Proceding of the Combustion Institute*, 15.

Okajima, S. and Kumagai, S. (1982). Experimental studies on combustion of fuel droplets in flowing air under zero- and high-gravity conditions. *Proceedings of the Combustion Institute*, 19.

Pope, D. N. and Gogos, G. (2005). A new multicomponent diffusion formulation for the finite-volume method: Application to convective droplet combustion. *Numerical Heat Transfer Part B-Fundamentals*, 48(3):213–233.

Raghavan, V., Pope, D. N., Howard, D., and Gogos, G. (2006). Surface tension effects during low-reynolds-number methanol droplet combustion. *Combustion and Flame*, 145(4):791–807.

Randolph, A. L., Makino, A., and Law, C. K. (1986). Liquid-phase diffusional resistance in multi-component droplet gasification. *Proceedings of the Combustion Institute*, 25:601–608.

Ranz, W. E. and Marshall, W. R. (1952). Evaporation from droplets. *Chem. Eng. Prog.*, 48:141–146 and 173–180.

Rex, J. F., Fuhs, A. E., and Penner, S. S. (1956). Interference effects during burning in air for stationary n-heptane, ethyl alcohol and methyl alcohol droplets. *Jet Propulsion*, 26:179–187.

Ronney, P. D. (1988). Understanding combustion processes through microgravity reaserch. *Proceedings of the Combustion Institute*, 22:2485–2506.

Sadhal, S. S. and Ayyaswamy, P. S. (1983). Flow past a liquid drop with a large non-uniform radial velocity. *Journal of Fluid Mechanics*, 133:65 – 81.

Sangiovanni, J. J. and Kesten, A. S. (1976). Effect of droplet interaction on ignition in monodispersed droplet streams. *Proceedings of the Combustion Institute*, 16:577–592.

Shaw, B. D. and Williams, F. A. (1990). Theory of influence of a low-volatility, soluble impurity on spherically symmetric combustion of fuel droplets. *International Journal of Heat and Mass Transfer*, 33:301–317.

Sirignano, W. A. (1993). Fluid dynamics of sparays - 1992 freeman scholar lecture. *ASME Jouranal of Fluid Engineering*, 1157:346–378.

Sirignano, W. A. (1999). *Fluid dynamics and transport of droplets and sprays*. Cambirdge University Press, England.

Smith, R. A., Wood, C. P., and Samuelsen, G. S. (1985). Formation of soot from practical land surrogate fuels in a swirl-stabilized, spray-atomized combustor. page 8, Monterey, CA, United States. Kinetic models;Surrogate fuels;Surrogate fuel kinetics;.

Spalding, D. B. (1953a). The combustion of liquid fuels. *Proceedings of the Combustion Institute*, 4:847–864.

Spalding, D. B. (1953b). Experiments on the burning and extinction of liquid fuel spheres. *Fuel*, 32:169–185.

Struk, P. M., T'ien, J. S., Dietrich, D. L., and d B Lenhert (1997). Experimental studies of flame shape around droplets in different buoyant environments. 35th Aerospace Sciences Meeting and Exhibit AIAA-97-1001, American Institute of Aeronautics and Astronautics.

Tsang, W. (2003). Experimental studies of flame shape around droplets in different buoyant environments. Technical Report NISTR-7155, National Institute of Standards and Technology.

Urban, D., Griffin, D., and Gard, M. (1997). In *NASA Fourth International Microgravity Combustion Workshop*, Cleveland, Ohio.

Waldman, C. H. (1974). Theory of non-steady state droplet combustion. *Proceedings of the Combustion Institute*, 15:429–442.

Wang, C. H., Liu, X. Q., and Law, C. K. (1984). Combustion and microexplosion of freely-falling multicomponent droplets. *Combustion and Flame*, 56:175–197.

Williams, A. (1973). Combustion of droplets of liquid fuels: A review. *Combustion and Flame*, 21:1–31.

Williams, F. A. (1960). On the assumptions underlying droplet vaporization and combustion. *Jouranal of Chemical Physics*, 33:133–144.

Williams, F. A. (1981). Droplet burning. In Cochran, T. H., editor, *Progress in Astronautics and Aeronautics*, volume 73, chapter 2, pages 31–60. American Institute of Aeronautics and Astronautics.

Williams, F. A. (1985). *Combustion Theory. 2^{nd} Edition.* Addison-Wesley, New York.

Williams, F. A. (2007). Contributions of microgravity research to adavancements in comustion science. In *Proceedings of the Sixth Asia-Pacific Conference on Combustion*, Nagoya Congress Center, Nagoya, Japan.

Wise, H. and Agoston, G. A. (1958). Burning of liquid droplets. In *Advances in Chemistry*, 20, pages 116–135. American Chemical Society, Washington, D.C.

Xiong, T. Y., Law, C. K., and Miyasaka, K. (1984). Interactive vaporization and combustion of binary droplet systems. *Proceedings of the Combustion Institute*, 20:1781–1787.

Yang, J. T., Wang, G. G., and Li, H. Y. (1990). Modeling of the convective thermal ignition process of solid fuel particles. *Journal of Heat Transfer*, 112:995–1001.

Zhang, H. R., Eddings, E. G., and Sarofim, A. F. (2007). Criteria for selection of components for surrogate of natural gas and transportation fuels. *Proceedings of the Combustion Institute*, 31:401 – 409.